

# We are IntechOpen, the world's leading publisher of Open Access books Built by scientists, for scientists

6,900

Open access books available

186,000

International authors and editors

200M

Downloads

Our authors are among the

154

Countries delivered to

TOP 1%

most cited scientists

12.2%

Contributors from top 500 universities



WEB OF SCIENCE™

Selection of our books indexed in the Book Citation Index  
in Web of Science™ Core Collection (BKCI)

Interested in publishing with us?  
Contact [book.department@intechopen.com](mailto:book.department@intechopen.com)

Numbers displayed above are based on latest data collected.  
For more information visit [www.intechopen.com](http://www.intechopen.com)



# Chirped-Pulse Oscillators: Route to the Energy-Scalable Femtosecond Pulses

Vladimir L. Kalashnikov

*Institut für Photonik, Technische Universität Wien  
Austria*

## 1. Introduction

In the last decade, femtosecond pulse technology has evolved extremely rapidly and allowed achieving a few-optical-cycle pulse generation directly from a solid-state oscillator (Brabec & Krausz (2000); Steinmeyer et al. (1999)). Applications of such pulses range from medicine and micro-machining to fundamental physics of light-matter interaction at unprecedented intensity level and time scale (Agostini & DiMauro (2004); Gattass & Mazur (2008); Hannaford (2005); Krausz & Ivanov (2009); Martin & Hynes (2003); Mourou et al. (2006); Pfeifer et al. (2006)). In particular, high-energy solid-state oscillators nowadays allow high-intensity experiments such as direct gas ionization (Liu et al. (2008)), where the level of intensity must be of the order of  $10^{14}$  W/cm<sup>2</sup>. Such an intensity level enables pump-probe diffraction experiments with electrons, direct high-harmonic generation in gases, production of nm-scale structures at a surface of transparent materials, etc. The required pulse energies have to exceed one and even tens of micro-joules at the fundamental MHz repetition rate of an oscillator (Südmeyer et al. (2008)).

Such energy frontiers have become achievable due to the chirped pulse amplification outside an oscillator (Diels & Rudolph (2006); Koechner (2006); Mourou et al. (2006)). However, the amplifier technology is i) complex, ii) expensive, iii) noise amplification is unavoidable, and iv) accessible pulse repetition rates lie within the kHz range. The last is especially important because the signal rates in, for example, electron experiments are usually low and an improvement factor of  $10^3$ – $10^4$  due to the higher repetition rate of the pulses significantly enhances the signal-to-noise ratio. Therefore, it is desirable to find a road to the direct over-microjoule femtosecond pulse generation at the MHz pulse repetition rates without an external amplification.

In principle, a cavity dumping allows increasing the pulse energy from a solid-state oscillator (Huber et al. (2003); Zhavoronkov et al. (2005)) but it makes the system more complex. There are the few alternative ways of increasing the oscillator pulse energy  $E$ , which is a product of the average power  $P_{av}$  and the repetition period  $T_{rep}$ : by increasing the cavity length and/or increasing the power (Apolonski et al. (2000); Cho et al. (1999); der Au et al. (2000); Südmeyer et al. (2008)). The impediment is that a high-energy pulse with  $E = P_{av}T_{rep}$  suffers from instabilities owing to nonlinear effects caused by the high pulse peak power  $P_0 \propto E/T$  ( $T$  is the pulse width). The leverage is to stretch a pulse, i.e. to increase its width  $T$  and thereby to decrease its peak power below the instability threshold.

One may grasp an implementation of this strategy on basis of the so-called solitonic conception of ultrashort pulse. If the pulse parameters change slowly during one cavity round-trip (that is a reasonable approximation for a typical solid-state oscillator), the ultrashort pulse can be treated as a dissipative soliton governed by both linear and nonlinear factors of an oscillator (Akhmediev & Ankiewicz (2005); Haus (1975a); Kärtner et al. (2004)). From a solitonic standpoint, the solid-state oscillators can be subdivided into i) those operating in the anomalous dispersion regime and ii) those operating in the normal dispersion regime.

In the anomalous dispersion regime, there are the simple relations between the pulse parameters  $E$ ,  $T$ , and  $P_0$  as well as the oscillator parameters  $\beta$  (that is the net-group-delay-dispersion coefficient) and  $\gamma$  (that is the self-phase modulation coefficient of a nonlinear medium, e.g. active crystal, air, optical plate, etc.) (Agrawal (2006))

$$T = \sqrt{|\beta|/\gamma P_0}, \quad E = 2|\beta|/\gamma T. \quad (1)$$

Since the peak power  $P_0$  has to be kept lower than some threshold value  $P_{th}$  in order to avoid the pulse destabilization, the energy scaling requires a pulse stretching which can be provided by only the substantial dispersion growth (see Eq. (1)):

$$E = 2\sqrt{P_{th}|\beta|/\gamma}. \quad (2)$$

In the normal dispersion regime, a pulse is stretched and its peak power is reduced due to appearance of the so-called chirp  $\psi$  (Haus et al. (1991)). The chirp means that the instantaneous frequency varies with time and, as a result, the pulse becomes stretched by  $\psi$  times in the time domain in comparison with a chirp-free pulse (Kharenko et al. (2011)). Since a pulse is chirped, an oscillator operating in such a regime is called as “chirped-pulse oscillator” (Fernández González (2008)). As a result of chirping, an oscillator becomes extremely stable at a comparatively low level of dispersion. The spectrally broad pulse from such an oscillator can be substantially compressed (the compression factor is  $\approx \psi$ ) with the proportional growth of its peak power  $P_0$ . An implementation of this regime promises a substantial enhancement of energy scalability in comparison with the law (2) and this strategy is the objective of the recent review.

The chapter is structured in the following way. In the first part, the physical principles of operation of a chirped-pulse oscillator are considered. The decisive contribution of dissipative effects such as the spectral filtering and the self-amplitude modulation into formation of a chirped-pulse is emphasized. Then, the concept of the chirped pulse as the chirped dissipative soliton is formulated. The underlying model is based on the so-called complex nonlinear Ginzburg-Landau equation (Akhmediev & Ankiewicz (1997); Aranson & Kramer (2002)). The main theoretical results concerning the chirped dissipative solitons of this equation are reviewed. They are based on both analytical and numerical integration techniques. The former can be divided into exact and approximated approaches. The last is most powerful and allows reducing the analysis of a chirped-pulse oscillator to the construction of two-dimensional “master diagram” comprising main properties of the chirped dissipative soliton (Kalashnikov et al. (2006)). The concept of the soliton energy scalability is analyzed and the different approaches to this concept are compared. In the course of analysis, a parallel between the chirped-pulse solid-state oscillators and the all-normal-dispersion fiber lasers (Rühl (2008); Wise et al. (2008)) is drawn.

In the last part of review some experimental achievements in the field of solid-state chirped-pulse oscillators are surveyed. Both broadband bulk and Yb:doped thin-disk oscillators are considered and the prospects for a further energy-scaling are estimated.

## 2. Operational principles and theory of chirped-pulse oscillators

In this section, the theory of a chirped-pulse oscillator will be outlined. As will be shown, the dissipative factors of a laser play a decisive role in the formation of an ultrashort pulse which can be treated as a chirped dissipative soliton. The underlying model is based on the complex nonlinear Ginzburg-Landau equation. Formulation and integration of this equation as well as interpretation of the obtained results are the important steps required for comprehension of the operational principles of chirped-pulse oscillators.

Firstly, we shall characterize the principal factors governing the oscillator dynamics and formulate the master equation (i.e. the complex nonlinear Ginzburg-Landau equation) modeling this dynamics. Then, the physical principles of the chirped pulse formation will be considered. It will be shown, that the chirped pulse exists due to a phase balance supported by a self-amplitude modulation. As a result, a chirped dissipative soliton emerges. Only two exact shapes for such a soliton are known. They are the partial solutions of the complex nonlinear Ginzburg-Landau equation and have a limited range of applications. Therefore, the approximated approaches to the master equation are of interest and they will be surveyed in a nutshell.

The first approach is based on the regularized adiabatic approximation (Ablowitz & Horikis (2009); Kalashnikov (2010); Podivilov & Kalashnikov (2005)) and the second class of approaches exploits the so-called Galerkin truncation (Blanchard & Brüning (1992); Malomed (2002)). The main advantage of the approximated methods is that they project the initial problem with infinitely many degrees of freedom to the finite-dimensional one that, thereby, makes the chirped dissipative soliton parameters to be easily traceable. We shall give emphasis to two practically important outputs of the approximated models of a chirped dissipative soliton viz. to the concepts of i) “master diagram” (Kalashnikov & Apolonski (2010); Kalashnikov et al. (2006)) and ii) “dissipative soliton resonance” (Chang et al. (2008b)). These concepts allow truncating the soliton parametrical space and provide the thorough grasp of the oscillator energy scalability. A possible application of the theory to the all-normal-dispersion fiber lasers will be implied in the course of consideration. In the course of this section, we shall touch upon some issues of a chirped-pulse oscillator stability.

### 2.1 Operational principles of a chirped-pulse oscillator

Let's begin with the consideration of principal factors governing the ultrashort pulse formation in an oscillator. Their schematic representation is shown in Fig. 1. In the slowly varying envelope approximation (Oughstun (2009)), the laser field envelope  $A$  evolves under influence of the operators corresponding to each of the factors represented in the diagram. The slowly varying envelope approximation is valid until  $T \gg 1/\omega_0$  and  $\Delta \ll \omega_0$  ( $\omega_0$  is the carrier frequency,  $\Delta$  is the spectral half-width of ultrashort pulse and  $T$  is its width) and has proved its usefulness for a theory of ultrashort pulse propagation even in the limit of  $T \rightarrow 1/\omega_0$  (Brabec & Krausz (1997)).

We shall consider below a  $(1 + 1)$ -dimensional field envelope  $A(z, \tau)$ , where  $z \in [0, NL_{cav}]$  is the propagation distance (i.e. the distance taken along the arrows in Fig. 1) and  $\tau \equiv [t -$

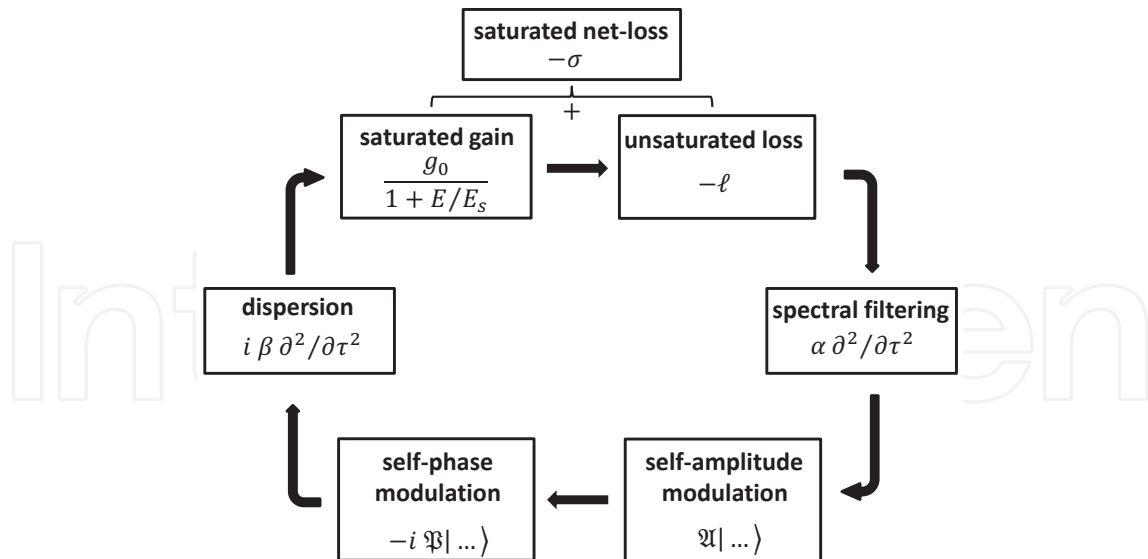


Fig. 1. Schematic representation of principal factors contributing to the ultrashort pulse formation and dynamics.

$z (dk/d\omega)|_{\omega=\omega_0} \in [0, T_{rep}]$  is the local or “reduced” time ( $t \in [0, NT_{rep}]$  is the time,  $\omega$  is the frequency deviation measured from  $\omega_0$ ,  $k(\omega)$  is the wave number). An oscillator is a naturally periodic system with the repetition time  $T_{rep} \equiv L_{cav}/c$  ( $c$  is the light speed,  $L_{cav}$  is the oscillator cavity length for a circular scheme of Fig. 1 or the double cavity length for a linear oscillator) and the repetition (“cavity round-trip”) number  $N$ .

### 2.1.1 Saturable gain and linear loss

The dissipative factors, which are generic for all types of oscillators, are the saturable gain and the linear (i.e. power-independent) loss. The latter includes both intracavity and output losses. In the simplest case, their common contribution into laser dynamics can be described as

$$\frac{\partial A(z, \tau)}{\partial z} = -\sigma A(z, \tau) = \frac{g_0 A(z, \tau)}{1 + E/E_s} - \ell A(z, \tau), \quad (3)$$

where  $g_0$  is the unsaturated gain defined by a pump (i.e. the gain coefficient for a small signal),  $E \equiv \int_0^{T_{rep}} |A|^2 d\tau$  is the intracavity field energy ( $|A|^2$  has a dimension of power),  $E_s \equiv \hbar\omega_0 S/\sigma_g$  is the gain saturation energy ( $\sigma_g$  is the gain cross-section and  $S$  is the laser beam area). Multiple propagation of the pulse through an active medium during one cavity round-trip, as it takes a place in a thin-disk oscillator (see Sec. 3) has to be taken into account by a corresponding multiplier before  $E$  in (3). The power-independent (“linear”) loss coefficient is  $\ell$ .

Since an oscillator in a steady-state regime operates in the vicinity of lasing threshold (where  $\sigma = 0$  by definition), one may expand  $\sigma$  (Kalashnikov et al. (2006)):

$$\sigma(E) \approx \delta \left( \frac{E}{E^*} - 1 \right), \quad (4)$$

where  $E^*$  is the energy of continuous-wave operation corresponding to  $\sigma = 0$ , and

$$\delta \equiv (d\sigma/dE)|_{E=E^*}.$$

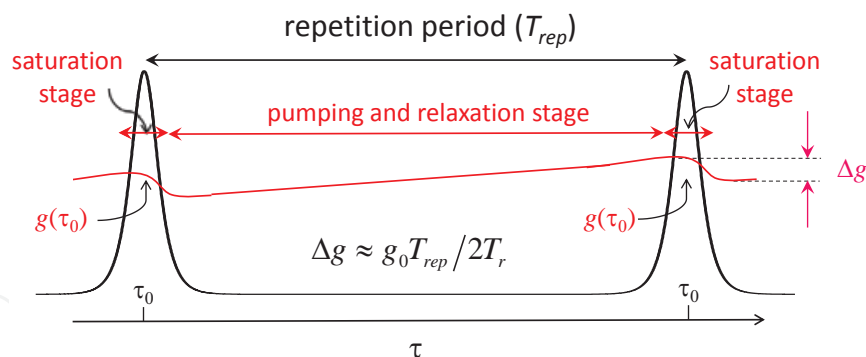


Fig. 2. Gain dynamics (red curve corresponds to  $g(\tau)$ ) affected by pumping, gain relaxation, and gain saturation in the steady-state (i.e.  $z$ -independent) pulsing regime (black curve corresponds to  $|A(\tau)|^2$ ).

Eqs. (3,4) do not take into account the time-dependence of  $\sigma$  due to the so-called dynamic gain saturation (see Fig. 2) (Kalashnikov (2008)). The dynamic gain saturation emerges when  $E/E_s \rightarrow 1$  and the gain is saturated by rather “fluent” energy  $\int_0^\tau |A|^2 d\tau'$ . For instance, a Ti:sapphire oscillator with  $S = 130 \mu\text{m}^2$  and  $E = 200 \text{ nJ}$  has  $E/E_s \approx 0.2$ . That is the dynamic gain saturation begins to play a role in the dynamics. In this case, Eq. (3) has to be supplemented with the rate equation for a four-level active medium (Herrmann & Wilhelm (1987)) that results in

$$\begin{aligned} \frac{\partial A(z, \tau)}{\partial z} &= (g(z, \tau) - \ell) A(z, \tau), \\ \frac{\partial g(z, \tau)}{\partial \tau} &= \frac{P_p}{S_p} \frac{\sigma_a}{\hbar\omega_a} (g_{\max} - g(z, \tau)) - \frac{|A(z, \tau)|^2}{SE_s} g(z, \tau) - \frac{g(z, \tau)}{T_r} \end{aligned} \quad (5)$$

Here the maximum gain  $g_{\max}$ , the absorption cross-section  $\sigma_a$ , the absorption frequency  $\omega_a$ , the absorbed pump power  $P_a$ , the pump beam area  $S_a$ , and the relaxation time  $T_r$ . For a pulse with  $T \ll T_{\text{rep}}$  (this requirement is trivial), one may use the expansion in  $E/E_s$ -series (Haus (1975b); Kalashnikov, Kalosha, Mikhailov, Poloyko, Demchuk, Koltchanov & Eichler (1995))

$$\sigma(z, \tau) = \ell - g(z, \tau_0) \exp\left(-\frac{\int_{\tau_0}^{T_{\text{rep}}} |A|^2 d\tau'}{E_s}\right) \approx \ell - g(z, \tau_0) \left(1 - \frac{\int_{\tau_0}^{T_{\text{rep}}} |A|^2 d\tau'}{E_s} + \dots\right). \quad (6)$$

Here  $g(\tau_0)$  is the gain at the pulse peak, which appears at some repetitive instant  $\tau \equiv \tau_0$  (Fig. 2).  $g(\tau_0)$  can be expressed iteratively by integration of the second equation of (5) (Jasapara et al. (2000)):

$$\begin{aligned} g(z, \tau_0) &= g_0 \left(z - cT_{\text{rep}}, \tau_0\right) \exp\left(-\frac{E}{2E_s} - \frac{T_{\text{rep}}}{T_r} - \frac{P_p}{S_p} \frac{\sigma_a T_{\text{rep}}}{\hbar\omega_a}\right) + \\ &+ \frac{g_{\max} P_p \sigma_a T_{\text{rep}} / S_p \hbar\omega_a}{E/2E_s + T_{\text{rep}}/T_r + P_p \sigma_a T_{\text{rep}} / S_p \hbar\omega_a} \left[1 - \exp\left(-\frac{T_{\text{rep}}}{T_r} - \frac{P_p}{S_p} \frac{\sigma_a T_{\text{rep}}}{\hbar\omega_a}\right)\right]. \end{aligned} \quad (7)$$

On the one hand, the contribution of  $\sigma(z, \tau)$  (Eqs. (3) or (5)) to the oscillator dynamics is important because the dissipative soliton emerges spontaneously from a destabilized continuous-wave regime of an oscillator (Soto-Crespo et al. (2002)). The continuous-wave solution of Eq. (3) corresponds to the condition  $\partial A/\partial z = -\sigma A = 0$ , which results in

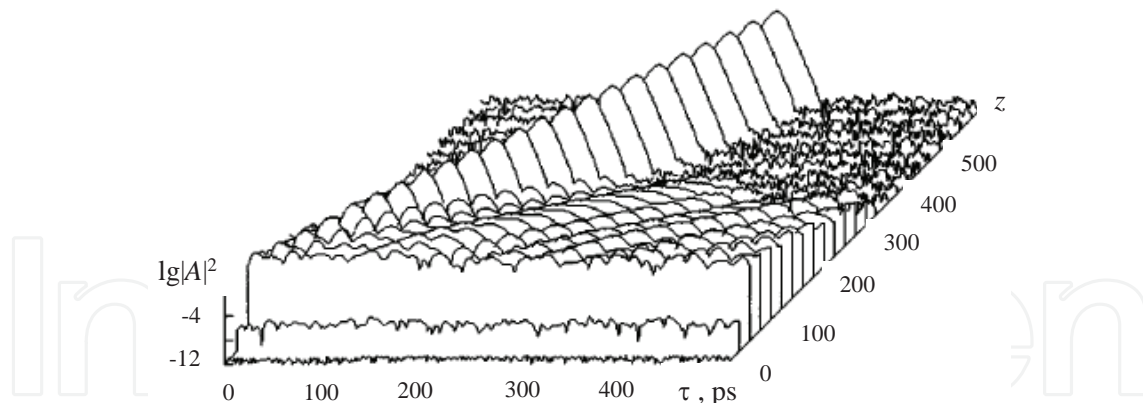


Fig. 3. Evolution of the normalized power for an oscillator studied in (Kalashnikov, Kalosha, Mikhailov & Poloyko (1995)). Figure illustrates the stages of ultrashort pulse formation with the initial noise amplification (vacuum instability), the continuous-wave formation, its destabilization, and the further noise reduction to an initial (“vacuum”) level at the stage, when a dissipative soliton becomes “mature”. The propagation distance  $z$  is normalized to  $cT_{rep}$ , i.e. it is the cavity round-trip number. Adapted from (Kalashnikov, Kalosha, Mikhailov & Poloyko (1995))

$P_{av} = 0$  (so-called “vacuum”), and  $P_{av} = E_s (g_0 - \ell) / \ell T_{rep}$  (actually, continuous-wave). The continuous-wave develops from the vacuum instability (the stage from  $z = 0$  to  $z \approx 100$  in Fig. 3).

On the other hand, the stability condition for the mature soliton is the vacuum stability that is  $\sigma > 0$ . This condition will play a crucial role in the sequel. It means physically that there exists no an amplification outside the dissipative soliton (see the stage after  $z \approx 300$  in Fig. 3, where the vacuum becomes stable). If the gain dynamics contributes (Fig. 2), such a criterion becomes even stronger (Kalashnikov et al. (2006)):

$$\sigma > \Delta g \approx g_0 T_{rep} / 2T_r. \quad (8)$$

Another important aspect of gain dynamics results from the energy-dependence of  $\sigma$  which causes a negative-feedback: the destabilizing growth (reduction) of soliton energy increases (decreases)  $\sigma > 0$  and, thereby, leads to the soliton attenuation (amplification) that tends in turn to the soliton stabilization.

### 2.1.2 Spectral filtering

As will be shown in Sec. 2.2, the spectral filtering is the key factor for a chirped-pulse oscillator. Such a filtering results from spectrally-dependent gain and/or loss and begins to contribute already at an initial stage of pulse formation. Fig. 3 demonstrates smoothing of an initial noise structure since the generation starts. In the spectral domain, a spectral filter provides a minimum loss at some frequency and, thereby, “selects” it (so-called “longitudinal mode selection”). The initially broad noise spectrum, corresponding to the short time spikes shrinks that corresponds to a smoothed time structure. The latter tends asymptotically to a continuous-wave. But a continuum-wave can be unstable in the presence of nonlinear factors (see next Sec. 2.1.3) so that an ultrashort pulse develops (Fig. 3).

Let us assume that a spectral filter has a profile  $\Phi(\omega)$ . Then, Eq. (3) has to be supplemented with

$$\frac{\partial A(z, \omega)}{\partial z} = \Phi(\omega) A(z, \omega), \quad (9)$$

where  $A(z, \omega)$  is the Fourier-image of  $A(z, \tau)$ .

Usually, the Lorentzian shape for  $\Phi(\omega)$  is assumed (Haus (1975a)):

$$\Phi(\omega) = \frac{g(\omega_0)}{1 + i\omega/\Omega}, \quad (10)$$

where  $g(\omega_0)$  is the gain coefficient or the maximum transmission coefficient (e.g., for an output mirror). It is assumed that spectral filtering is centered at  $\omega_0$ .  $\Omega$  is the filter bandwidth.

If  $2\Delta \ll \Omega$ , one may expand (10) and proceed in the time-domain

$$\frac{\partial A(z, \tau)}{\partial z} \approx g(\omega_0) \left[ 1 - \frac{1}{\Omega} \frac{\partial}{\partial \tau} + \frac{1}{\Omega^2} \frac{\partial^2}{\partial \tau^2} - h.o.t. \right] A(z, \tau), \quad (11)$$

where *h.o.t.* means the higher in  $\partial/\partial\tau$ -order terms, which are negligible as a rule (for some important exceptions see, e.g. (Akhmediev & Ankiewicz (2005); Kalashnikov et al. (2011))).

### 2.1.3 Self-amplitude modulation

A self-amplitude modulation provides a pulse-power discrimination so that the net-gain increases with  $|A|^2$  (at least up to some power level). This factor forms and stabilizes a pulse (Fig. 3). The mechanisms of self-amplitude modulation are various (Paschotta (2008); Weiner (2009)) but there are two ones, which are widespread in the solid-state oscillators: i) Kerr-lens mode-locking (KLM) (Spence et al. (1991)), and ii) mode-locking due to a semiconductor saturable absorber mirror (SESAM) (Keller et al. (1996)).

The KLM uses a self-focusing of laser beam inside some nonlinear element (e.g., active medium) that changes diffractive loss (so-called hard aperture mode-locking) or overlapping between the lasing and pumping beams (so-called soft aperture mode-locking) (Paschotta (2008)). It is important, that i) response of this mechanism to a laser field is practically instantaneous (i.e. it is power-dependent), and ii) the mechanism is strongly interrelated with the self-phase modulation (see next Sec. 2.1.4) because both phenomena are caused by the same nonlinear process.

A detailed modeling of spatial variations of laser beam is cumbersome and unpractical. Therefore, some reduction of dimensionality is required. For instance, one may consider an evolution of only zero-order Gaussian beams under action of factors presented in Fig. 1 (Kalashnikov, Kalosha, Mikhailov & Poloyko (1995); Kalosha et al. (1998)). However, such an approach remains to be cumbersome because it needs considering the detailed geometrical structure of an oscillator. Hence, it is usable to reduce the KLM to an action of some effective fast saturable absorber with a response function  $\mathfrak{U}|A(z, \tau)\rangle \equiv \mathfrak{F}(|A(z, \tau)|^2)A(z, \tau)$  so that Eqs. (3,9) have to be supplemented with

$$\frac{\partial A(z, \tau)}{\partial z} = \mathfrak{F}(|A(z, \tau)|^2)A(z, \tau). \quad (12)$$

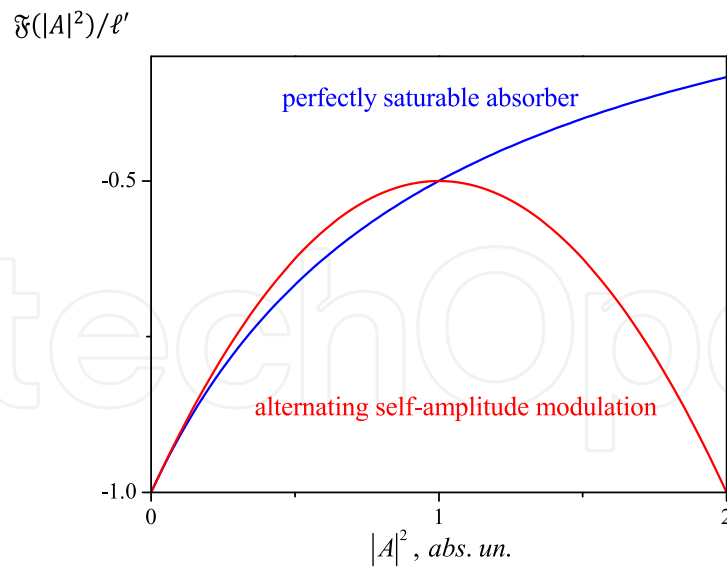


Fig. 4. Idealized self-amplitude modulation functions  $\mathfrak{F}(|A(z, \tau)|^2)$ .

From this point of view, one may consider the soft and hard aperture mode-locking as (see Fig. 4) i) “alternating” self-amplitude modulation for the former with

$$\mathfrak{F}(|A(z, \tau)|^2) \approx -\ell' + \kappa(1 - \zeta|A(z, \tau)|^2)|A(z, \tau)|^2, \quad (13)$$

where a loss saturation changes into a loss enhancement with the power growth; and ii) perfectly saturable absorber for the latter with

$$\mathfrak{F}(|A(z, \tau)|^2) \approx -\frac{\ell'}{1 + \kappa|A(z, \tau)|^2}, \quad (14)$$

where the loss  $\ell'$  vanishes asymptotically with the power growth.

Here  $\ell'$  is the low-power saturable loss (i.e. unsaturated saturable loss) and it has not to be confused with  $\ell$  (i.e. unsaturable loss). The  $\ell'$ -coefficient can be absorbed by  $\sigma$  (Eq. 3) (for such “absorption”, the right-hand side of Eq. 14 has to be rewritten as

$-\ell' + \ell'\kappa|A|^2 / (1 + \kappa|A|^2)$ ). The  $\kappa$ -parameter is the self-amplitude modulation coefficient (i.e. the inverse power of loss saturation),  $\zeta$  is the coefficient of self-amplitude alteration.

Physical sense of the curves presented in Fig. 4 can be explained in the following way. Self-focusing inside a nonlinear element is provided by the cubic nonlinearity therefore the leading term in (12) is proportional to  $|A|^2A$ . If a hard aperture is used, the beam squeezing due to self-focusing leads to the monotonic decrease of the diffraction loss (Eq. (14) and the blue curve in Fig. 4). If a soft aperture is used, the overlapping between the lasing and pumping beams and, thereby, the gain increases initially with power. Then the overlapping becomes complete and the gain reaches its maximum. Further growth of power worsens the overlapping and the gain decreases with power (Eq. (13) and the red curve in Fig. 4).

Now let's consider a SESAM as the self-amplitude modulator. As a rule, the nonlinear properties of a semiconductor structure are complex. Despite this complexity, one may model the nonlinear response of a SESAM by Eq. (12) if  $T \gg T_r^E$  ( $T_r^E$  is the decomposition time of

excitons which is lesser than 100 fs as a rule) and  $T_r^E \ll T_r^F$  ( $T_r^F$  is the recombination time of free carriers which exceeds tens of picoseconds) (Haus & Silberberg (1985)). Then,  $\ell'$  is the modulation depth, and  $\kappa \equiv 2\sigma^A T_r^E / \hbar\omega_0 S_A$  is the inverse saturation power of absorber ( $S_A$  is the beam area on an absorber,  $\sigma^A$  is the absorption cross-section). Since  $T$  equals to a few of picoseconds for an uncompressed chirped pulse, the approximation  $T \gg T_r^E$  is quite precise for a chirped-pulse oscillator.

#### 2.1.4 Self-phase modulation

Active crystal, air, optical plates, etc. have a third-order nonlinearity so that their refractivity indexes  $n$  are power-dependent:  $n = n_0 + \gamma|A|^2$  ( $n_0$  is the refractive index for a small signal,  $\gamma$  is the self-phase modulation coefficient for a medium) (Agrawal (2006)). The coefficient  $\gamma$  can be estimated as:  $\gamma = 8\pi^2 n_0 n_2 / \lambda^2$  for the case of strong beam focusing inside a nonlinear element (e.g. inside an active crystal or optical plate) or  $\gamma = 4\pi n_2 L / \lambda S$  for the case of weak focusing (e.g. inside an active thin-disk or air) (Weiner (2009)). Here  $\lambda$  is the central wavelength of an oscillator,  $L$  is the length of a nonlinear medium,  $n_2$  is its nonlinear refractive index, and  $S$  is the beam area.

Since the  $\gamma$ -coefficient depends on beam area in the last formula, the self-focusing can affect the self-phase modulation through the  $S$ -change. As a result, the refractive index acquires the corrections with higher-order powers of  $|A|$ . Then, the contribution of self-phase modulation can be modeled as

$$\frac{\partial A(z, \tau)}{\partial z} = -i\mathfrak{P} |A(z, \tau)| = -i \left[ \gamma + \chi |A(z, \tau)|^2 \right] |A(z, \tau)|^2 A(z, \tau), \quad (15)$$

where  $\chi$  describes the higher-order correction to the self-phase modulation coefficient.

Despite the factors considered above, the self-phase modulation is non-dissipative effect and does not change the pulse energy.

#### 2.1.5 Group-delay dispersion

The last effect required for the ultrashort pulse generation is the group-delay dispersion. This effect causes frequency dependence of the wave propagation constant  $k$ :  $k(\omega) = k(\omega_0) + k_1\omega + k_2\omega^2 + h.o.t.$  Since an ultrashort pulse has a broad spectrum, such a dependence cannot be neglected. The coefficients  $k$  and  $k_1$  can be included in the definitions of the soliton wave-number and the reduced time  $\tau$ , respectively. Then, the contribution of the group-delay dispersion is defined as

$$\frac{\partial A(z, \tau)}{\partial z} = i\beta \frac{\partial^2 A(z, \tau)}{\partial \tau^2} + h.o.t. \quad (16)$$

Here  $\beta \equiv L_{cav} (dk/d\omega)|_{\omega=\omega_0}$  is the group-delay dispersion coefficient and, in our notations, it is positive for a normal dispersion and negative for an anomalous dispersion.

Both self-phase modulation and group-delay dispersion are non-dissipative effects and contribute to the pulse phase profile. In the solitonic regime, these contributions have to be balanced therefore both  $\gamma$  and  $\beta$  are the key control parameters of an oscillator.

Higher-order terms in (16) are called as the higher-order dispersions and become especially important for broadband oscillators (such as Ti:sapphire, Cr:YAG, Cr:ZnSe, etc.). Some aspects

of their contribution to the characteristics of a chirped-pulse oscillator will be considered in Sec. 2.3.1, as well.

### 2.1.6 Haus master equation

The pulse changes during one cavity round-trip are, as a rule, small for a solid-state oscillator. That allows joining Eqs. (3,11,12,15,16):

$$\frac{\partial A(z, \tau)}{\partial z} = \left[ -\sigma(E) + \frac{g(\omega_0)}{\Omega^2} \frac{\partial^2}{\partial \tau^2} + \mathfrak{F}(|A|^2) \right] A(z, \tau) + i \left\{ \beta \frac{\partial^2}{\partial \tau^2} - \gamma |A|^2 - \chi |A|^4 \right\} A(z, \tau). \quad (17)$$

Eq. (17) is the modified Haus master equation introduced in (Haus et al. (1991)). Formally, it can be rated as a complex nonlinear Ginzburg-Landau equation (Akhmediev & Ankiewicz (1997); Aranson & Kramer (2002)). The last has an extremely wide horizon of applications covering quantum optics, modeling of Bose-Einstein condensation, condensate-matter physics, study of non-equilibrium phenomena, and nonlinear dynamics, quantum mechanics of self-organizing dissipative systems, and quantum field theory. In laser physics, this equation provides an adequate description of ultrashort pulses in both solid-state (Haus et al. (1991)) and fiber (Ding & Kutz (2009); Komarov et al. (2005)) lasers, as well as, pulse propagation in nonlinear fibers. As will be shown in Sec. 2.3, the theory of chirped-pulse oscillators is based mainly on study of soliton-like solutions of (17). Hereinafter, we shall attend to two main modifications of (17): i) cubic-quintic nonlinear Ginzburg-Landau equation (CQNGLE) with  $\mathfrak{F}(|A(z, \tau)|^2)$  defined by (13), and ii) generalized nonlinear Ginzburg-Landau equation (GNGLE) with  $\mathfrak{F}(|A(z, \tau)|^2)$  defined by (14).

The exact analytical solutions of the complex nonlinear Ginzburg-Landau equation are known only for a few of cases, when they represent the dissipative solitons and some algebraic relations on the parameters of the equation are imposed (Akhmediev & Afanasjev (1996)). More general solutions can be revealed on basis of the algebraic nonperturbative techniques (Conte (1999)), which, nevertheless, are not developed sufficiently still. The perturbative methods allow obtaining the dissipative soliton solutions (Malomed & Nepomnyashchy (1990)) in the vicinity of the Schrödinger solitonic sector (Agrawal (2006)) of CQNGLE. Another approximate methods utilize the reduction of infinite-dimensional space of CQNGLE to the finite-dimensional one on basis of the method of moments (Tsoy & Akhmediev (2005)) or the variational method (Ankiewicz et al. (2007); Bale & Kutz (2008)). At last, there is the direct approximate integration technique for the complex Ginzburg-Landau equation with an arbitrary  $\mathfrak{F}(|A(z, \tau)|^2)$  (Podivilov & Kalashnikov (2005)). Applications of these methods to the theory of chirped-pulse oscillator will be reviewed in Sec. 2.3.

## 2.2 Physical principles of chirped dissipative soliton formation

A dissipative soliton is named as “chirped” one if its phase  $\phi(\tau)$  is time-dependent. The chirp results from a joint action of normal dispersion ( $\beta > 0$ ) and self-phase modulation. Eq. (17) suggests that a round-trip contribution of the time-dependent phase to the pulse phase change is  $-\beta |A(\tau)| [d\phi(\tau)/d\tau]^2 - \gamma |A(\tau)|^3$  (blue curve in left Fig. 5). Simultaneously, a phase contribution of the pulse envelope is  $\beta \partial^2 |A(\tau)| / \partial \tau^2$  (red curve in left Fig. 5). Hence, the phase balance is *possible* for a chirped pulse propagating in the normal dispersion regime (Kalashnikov et al. (2008); Renninger et al. (2011)). It should be noted, that the Schrödinger

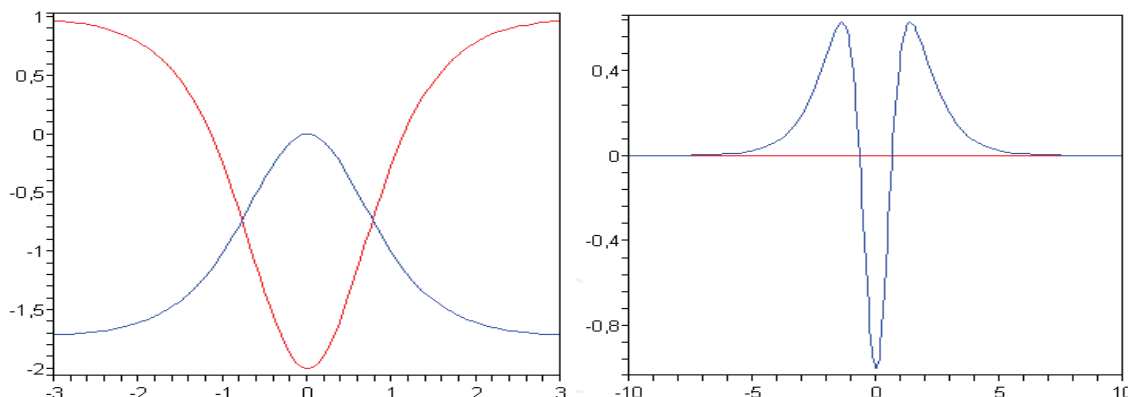


Fig. 5. One cavity round-trip contribution to the time-dependent phase  $\phi(\tau)$  (left) and the amplitude  $|A(\tau)|$  (right) for a chirped pulse. Left: the blue curve corresponds to contribution from the time-dependent phase, the red curve corresponds to contribution from the pulse envelope. The horizontal axes correspond to  $\tau$  in arb. un.

soliton (Agrawal (2006)) developing in the anomalous dispersion regime ( $\beta < 0$ ) exists owing to a phase balance, which is possible only in the absence of chirp.

The simple condition for a phase balance can be expressed as  $\psi^2 = 2 + \gamma P_0 T^2 / \beta$  if  $A(\tau) = \sqrt{P_0} \text{sech}(\tau/T)^{1+i\psi}$  ( $\psi$  is the chirp parameter, i.e.  $\phi(\tau) = \psi \ln[\text{sech}(\tau/T)]$ ),  $g(\omega_0)/\Omega^2 \beta \ll 1$ , and  $\chi = 0$ .

However unlike the Schrödinger soliton, the only phase balance is not sufficient for a chirped dissipative soliton existence. There is the amplitude perturbation (right Fig. 5) causing the soliton spreading. The source of this perturbation is the time-dependent phase, which contributes through a dispersion:  $-\beta [2 (dA(\tau)/d\tau) (d\phi(\tau)/d\tau) + A(\tau) (d^2\phi(\tau)/d\tau^2)]$ . In addition, there exists a dissipation owing to spectral filtering  $(g(\omega_0)/\Omega^2) d^2 |A(\tau)|/d\tau^2$  and a net-loss with the coefficient  $\sigma > 0$  (see Eq. (17)). Hence, some self-amplitude modulation is required for the soliton stabilization.

The obvious mechanism, which acts against the pulse spreading and dissipation is the nonlinear gain provided by  $\mathfrak{F}(|A(z, \tau)|^2)$ . But for a chirped pulse, there exists an additional squeezing mechanism resulted from the spectral filtering and defined by the term

$$- (g(\omega_0)/\Omega^2) |A(\tau)| (d\phi(\tau)/d\tau)^2 \text{ in Eq. (17).}$$

Physically, the action of the last mechanism can be explained in the following way (see (Haus et al. (1991); Proctor et al. (1993))). The chirp causes the substantial spectral broadening so that  $T\Delta \gg 1$  (see left Fig. 6, where the Wigner function (Diels & Rudolph (2006)) for a chirped pulse is shown). As a result of such broadening, the spectral filtering becomes conspicuous. It cuts off the spectral components located at the pulse wings (right Fig. 6) that results in the pulse shortening. Thus, the balance of both dissipative and non-dissipative factors can support the self-sustained ultrashort pulse in a chirped-pulse oscillator. The theory of such self-sustained pulse, or “chirped dissipative soliton”, will be considered below.

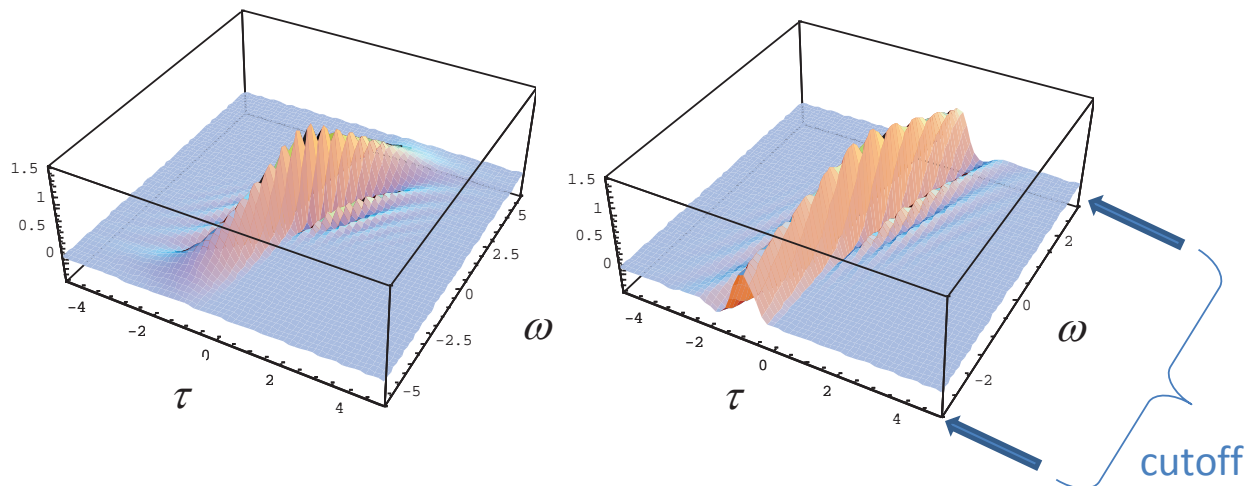


Fig. 6. Left: the Wigner function of a chirped pulse (arb. un.). Right: spectral cut-off resulting in the pulse shortening.

### 2.3 Theory of chirped dissipative soliton

It is convenient to systemize the theory of chirped-pulse oscillators from the point of view of approaches based on the concept of a chirped dissipative soliton. Such approaches can be divided into i) numerical, ii) exact analytical, and iii) approximated analytical ones. Of course, this division is conventional and a realistic analysis combines different approaches, as a rule.

#### 2.3.1 Numerical modeling of chirped dissipative soliton

The master equation (17) is multiparametrical and the direct numerical simulations face the challenge of coverage of a multidimensional parametrical space. That requires the extensive calculations and the obtained results have to be carefully sorted. Moreover, the real parametrical space of a chirped dissipative soliton can differ from a separate set of the independent parameters of (17). In this case, the numerical identification of a relevant parametrical space is intricate problem. Nevertheless, a numerical approach provides most complete and adequate description of a real-world oscillator. In particular, such important characteristics of a mode-locked oscillator as its stability and self-starting ability, allocation of laser elements and noise properties can be analyzed mainly numerically. In addition, the numerical simulations are the testbed for any analytical model.

Extensive numerical simulations of the CQNGLE in the normal dispersion regime, that is relevant for the theory of chirped-pulse oscillator, have been carried out by N.N. Akhmediev with coauthors (Akhmediev et al. (2008); Soto-Crespo et al. (1997)). The simulations have allowed finding the pulse stability regions for some two-dimensional projections of the CQNGLE parametrical space. Unfortunately, the problem is that these regions cannot be compared directly with a parametrical space of concrete oscillator generally owing to dropping of the energy-dependence of net-loss parameter  $\sigma$  (i.e.  $\delta$ -parameter in the notations of (Akhmediev et al. (2008); Soto-Crespo et al. (1997))). Additionally, the energy belongs rather to a set of control parameters of an oscillator than it is some derivative parameter of a solitonic solution.

Nevertheless, the numerical results of (Akhmediev et al. (2008); Soto-Crespo et al. (1997)) provide the qualitative grasp of the dissipative soliton properties. Fig. 7 demonstrates

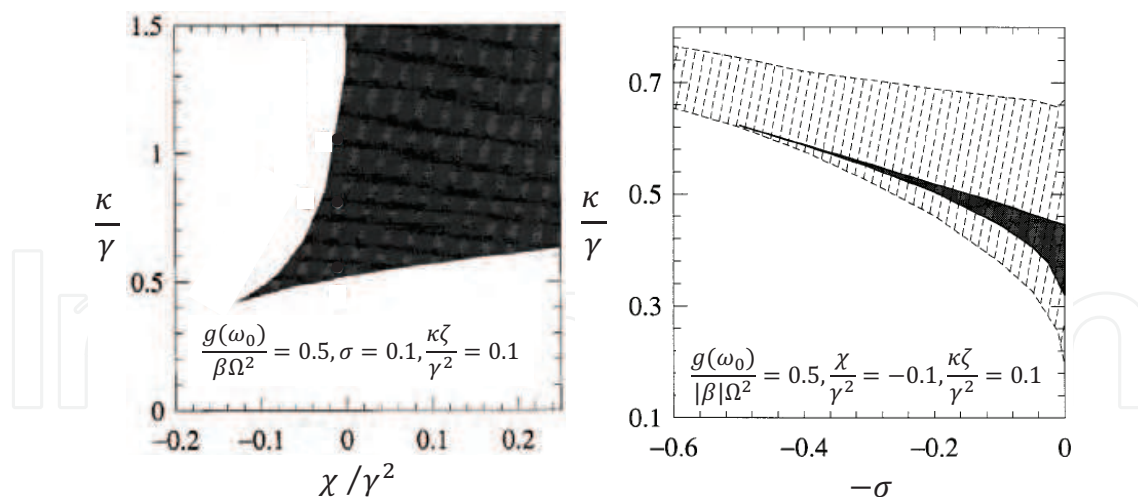


Fig. 7. Regions where the stable dissipative solitons exist in the normal dispersion regime (filled). For comparison, the hatched region in the right figure corresponds to the soliton developing in the anomalous dispersion regime. The parameters correspond to Eqs. (13,17). Adapted from (Soto-Crespo et al. (1997)).

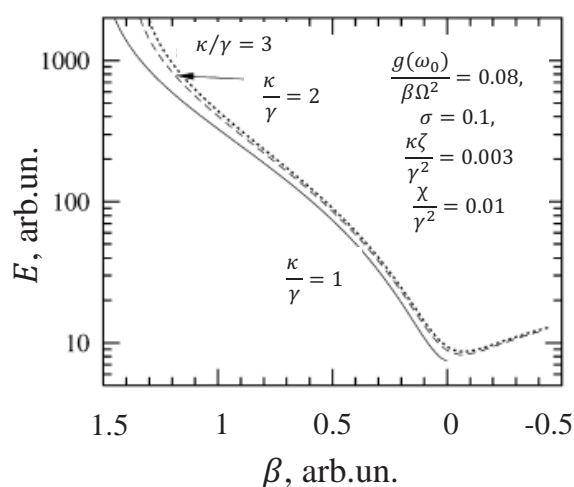


Fig. 8. Soliton energy versus dispersion  $\beta$ . Adapted from (Akhmediev et al. (2008)).

the numerically calculated regions where the stable dissipative solitons of Eqs. (13,17) exist (Soto-Crespo et al. (1997)). One may see (left figure) that the self-limited self-phase modulation ( $\chi < 0$ ) tends to destabilize the dissipative soliton (the stability region shrinks). The right Fig. 7 demonstrates another interesting property: the *isogain* region (i.e. the region of pulse existence where  $\sigma = \text{const}$ ) is strongly confined in the  $\kappa$ -dimension. The dissipative solitons with such properties will be called the *positive-branch* solitons (the sense of this term will be clear in sequel).

The physically important property of the positive-branch dissipative soliton is the swift growth of its energy along an isogain with the dispersion  $\beta$ . It means that such a soliton is *energy scalable* (see Fig. 8). Simultaneously, the energy dependence on the self-amplitude parameter  $\kappa$  is weaker. As will be shown in Secs. 2.3.2.2 and 2.3.2.3, such scaling properties of chirped-pulse oscillator can be explained on the basis of analytical approaches.

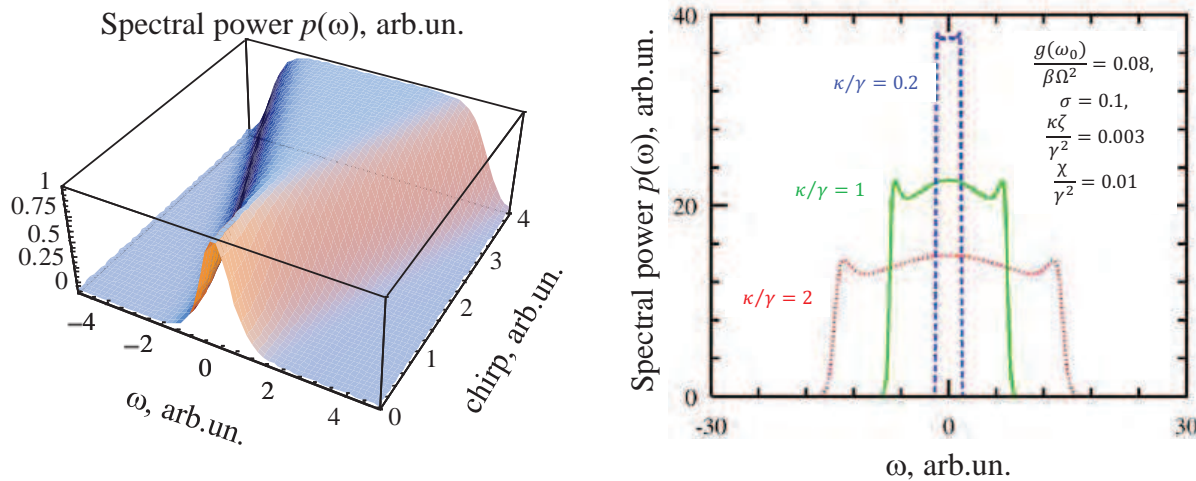


Fig. 9. Chirped dissipative soliton spectra. Left: spectrum vs. chirp parameter  $\psi$  for a chirped soliton  $\sqrt{P_0}\text{sech}(\tau/T)^{1+i\psi}$ . Right: spectra of the CQNGLE solitons adapted from (Akhmediev et al. (2008)).

The remarkable feature of a chirped-pulse oscillator is that its spectrum, which broadens with a chirp, has truncated edges (left Fig. 9) and flat, concave, convex and concave-convex tops (left and right Figs. 9, see also (Chong et al. (2008a); Kalashnikov et al. (2006; 2005))). The last spectral type has a modification with sharp spikes at the spectrum edges (Chong et al. (2008a); Kalashnikov & Chernykh (2007)).

The truncated spectral shape results from a rapid chirp growth at the spectrum edges (Kalashnikov et al. (2005)). Simultaneously, a chirp growing with dispersion causes the pulse stretching and, thereby, reduces its peak power that prevents the soliton destabilization (Chong et al. (2008a); Kalashnikov et al. (2006; 2005); Soto-Crespo et al. (1997)). Such a stretched pulse can be dechirped and compressed outside an oscillator cavity by approximately factor of  $\psi$ , where  $\psi$  is the dimensionless chirp parameter:  $\psi \approx T\Delta/4 \approx (1/4)d^2\phi(\omega)/d\omega^2$  ( $T$  is the soliton width before compression,  $\Delta$  is the soliton spectral half-width,  $\phi(\omega)$  is the spectral phase) (Kalashnikov et al. (2005)). The  $\psi$ -value can be estimated approximately as

$$\psi \approx \frac{3}{(g(\omega_0)/\Omega^2\beta) + (\kappa/\gamma)}, \quad (18)$$

which explains the chirp growth with dispersion ( $\beta$ ), self-phase modulation ( $\gamma$ ), and broadening of a spectral filter ( $\Omega$ ).

Since the spectral chirp increases abruptly at spectrum edges, the satellites appear at the soliton wings after dechirping. Such satellites have uncompensated chirp, large frequency deviation and contain a part ( $\approx 10\%$ ) of full energy (Kalashnikov et al. (2005)).

Numerical simulations demonstrate the spectral broadening with the dispersion decrease (Chong et al. (2008a); Kalashnikov et al. (2006; 2005)) although some spectral width reduction can appear for the small normal dispersions (Soto-Crespo et al. (1997)). Also, a spectrum broadens with a growth of the nonlinear phase shift and the spectral filtering (Chong et al. (2008a)). The pulse energy increases with the nonlinear phase shift (Chong et al. (2008a)) and dispersion (Kalashnikov et al. (2006; 2005); Soto-Crespo et al. (1997)).

Variety of the numerical results allows identifying the control parameters of a chirped-pulse oscillator with  $\beta$  (dispersion),  $\Omega$  (spectral width of filter or gainband),  $\gamma$  (self-phase modulation coefficient), and  $\kappa$  (coefficient of self-amplitude modulation) (see Eqs. (13,17)) and conjecturing that their dimensionless combination in the form of (Kalashnikov et al. (2006))

$$C \equiv \frac{g(\omega_0)}{\beta \Omega^2} \frac{\gamma}{\kappa} = \frac{\alpha}{\beta} \frac{\gamma}{\kappa} \quad (19)$$

is relevant to the description of the dissipative soliton properties (the abbreviation  $\alpha \equiv g(\omega_0)/\Omega^2$  is introduced). Such a conjecture is suggested by the analytical theory as well (see Secs. 2.3.2.2 and 2.3.2.3) and gives a deep insight into the properties of chirped-pulse oscillators. The most important understanding is that the properties of chirped dissipative soliton are defined primarily by not absolute values of parameters but their relations: spectral dissipation to dispersion and self-phase modulation to self-amplitude one. This observation allows a unified standpoint at the very different lasers operating in the normal dispersion regime. For instance, the fiber lasers operate on comparatively high levels of dispersion ( $\approx 0.01 \div 0.1 \text{ ps}^2$ ) but the self-phase modulation is high, as well. As a result, the C-parameter does not differ substantially from that for a solid-state oscillator. This allows including the fiber lasers into consideration (e.g. see works of F. Wise with coauthors).

The detailed analysis of this topic will be presented in Secs. 2.3.2.2 and 2.3.2.3 but it should be noted here that the relevance of combined parameters like C suggests the existence of low-dimensional hyper-surfaces in a multidimensional parametrical space of dissipative soliton which characterizes both solid-state and fiber lasers. The important examples of such low-dimensional parametrical representations of a dissipative soliton are based on the closely related concepts of the “*master diagram*” (Kalashnikov et al. (2006)) (Fig. 10) and the “*dissipative soliton resonance*” (Chang et al. (2008b)) (Fig. 11). It has been demonstrated, that both master diagram and dissipative soliton resonance are sufficiently robust structures and remain in the oscillators with a parameter management (Chang et al. (2008a); Kalashnikov et al. (2006)).

Significance and structure of the master diagram will be described in detail in Secs. 2.3.2.2 and 2.3.2.3 but one has to note here that the isogains (i.e. curves with  $\sigma = \text{const}$ ) play a special role in the structure of representations of Figs. 10,11 (e.g., see (Bélanger (2007))). In particular, the singular curve  $\sigma = 0$  denotes the soliton stability threshold. It was found numerically that the net-loss parameter  $\sigma$  increases almost linearly with  $\kappa/\gamma$  (Kalashnikov et al. (2005)). Also, this parameter increases initially with the dispersion lowering but then it decreases and approaches zero (Fig. 12). Really, the soliton loses its stability at some  $\sigma = \Delta g > 0$  (Eq. (8)) due to dynamic gain saturation. The loss of stability means that the noise out of the pulse begins to amplify.

This observation testifies that the saturable gain is the decisive factor in a pulse stabilization. As has been found (Kalashnikov & Chernykh (2007); Kalashnikov et al. (2006)), the energy-dependence of  $\sigma$  is required to stabilize a chirped dissipative soliton so that some types of chirped dissipative solitons lose a stability in the absence of gain saturation (Kharenko et al. (2011)). Simultaneously, the gain dynamics during one cavity round-trip (so-called dynamic gain saturation, see Eq. (5)) can cause a soliton destabilization. Numerical simulations of (Kalashnikov (2008)) suggest that the stability region becomes confined on the (*Pump–Dispersion*)-plane in the presence of dynamic gain saturation. This means that there are some minimum and maximum dispersions as well as minimum and maximum pump

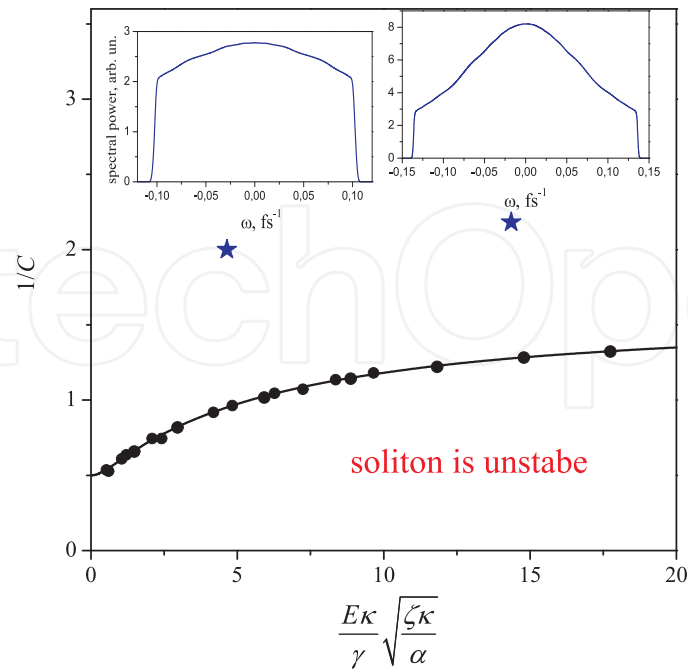


Fig. 10. The master diagram adapted from (Kalashnikov et al. (2006)). The circles obtained from simulations of a Ti:sapphire oscillator correspond to the isogain  $\sigma = 0$ . The numerical spectra (inserts) are placed in vicinity of the corresponding parametrical points (blue stars).

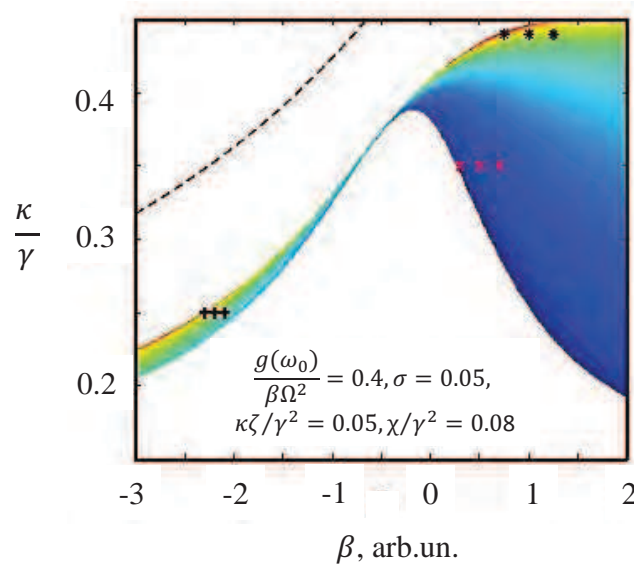


Fig. 11. Contour plot of the energy of stable soliton solution of the CQNGLE in the two-dimensional parameter space of dispersion  $\beta$  and nonlinear gain  $\kappa$ . Color scales the pulse energy from low (blue) to high (red) levels. The dashed line is an analytical approximation to the resonance curve (Chang et al. (2008b)). Adapted from (Grelu et al. (2010)).

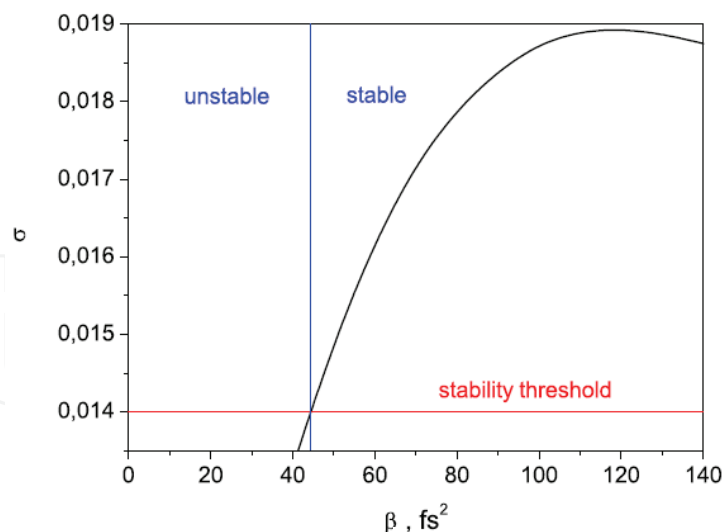


Fig. 12. Dependence of the net-loss parameter  $\sigma$  on dispersion. The stability threshold ( $\sigma_{th}$ ) is determined by the dynamic gain saturation. Adapted from (Kalashnikov et al. (2005)).

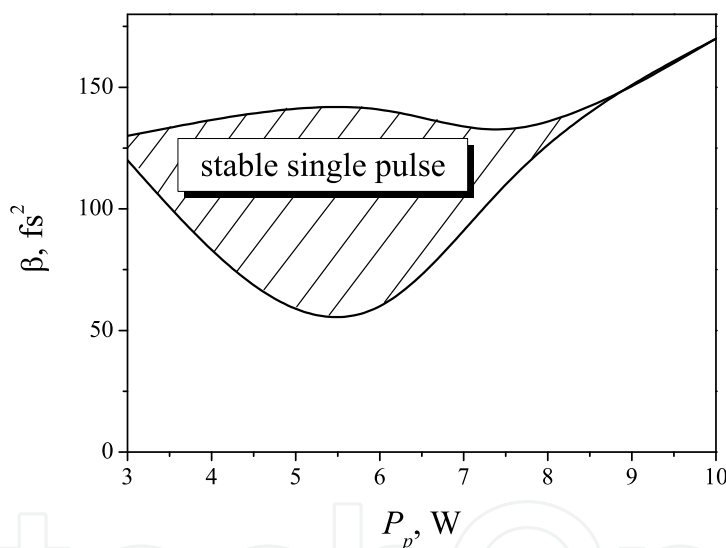


Fig. 13. Region of the chirped dissipative soliton stability (shaded area) in the presence of dynamic gain saturation (Eqs. (5,13,17)) with  $\zeta = 0.6\gamma$ ,  $\kappa = 0.04\gamma$ ,  $g_{max} = 0.33$ ,  $\ell = 0.22$ ,  $S_p = 100 \mu\text{m}^2$ ,  $S = 130 \mu\text{m}^2$ ,  $T_r = 3.5 \mu\text{s}$ . Double transit through a Ti:sapphire crystal per one round-trip ( $T_{rep} = 21 \text{ ns}$ ) was considered. Adapted from (Kalashnikov (2008)).

powers providing a stable pulse (Fig. 13). The destabilizing mechanism was identified with an appearance of satellite in front of the pulse that results from the dynamic gain saturation and causes the energy transfer from a pulse to a satellite.

A special problem, which can be explored chiefly numerically is the stability of a chirped-pulse oscillator against the higher-order dispersions, i.e. in the presence of a frequency-dependence of the dispersion coefficient  $\beta(\omega)$ . Such a dependence is substantial in broadband chirped-pulse oscillators like Ti:sapphire (Kalashnikov et al. (2005)), Cr:YAG (Sorokin et al. (2008)) and Cr:ZnSe (Kalashnikov et al. (2011)). As a result, the master equation (17) has to

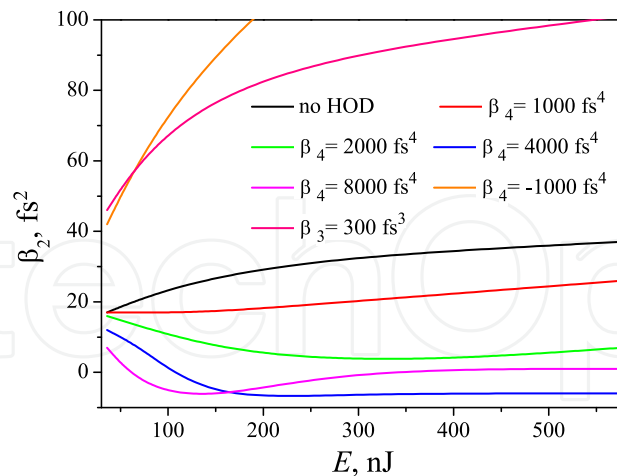


Fig. 14. Dependence of the stability threshold on the energy and a higher-order dispersion (HOD). Adapted from (Kalashnikov et al. (2008)).

be modified so that (e.g., see (Kalashnikov et al. (2008)))

$$\frac{\partial A(z, \tau)}{\partial z} = \left[ -\sigma(E) + \frac{g(\omega_0)}{\Omega^2} \frac{\partial^2}{\partial \tau^2} + \mathfrak{F}(|A|^2) \right] A(z, \tau) + i \left\{ -\sum_{n=2}^N i^n \beta_n \frac{\partial^n}{\partial t^n} - \gamma |A|^2 - \chi |A|^4 \right\} A(z, \tau), \quad (20)$$

where  $\beta_n$  are the dispersion coefficients of  $n^{\text{th}}$ -order.

The results of simulations for a Ti:sapphire oscillator with  $N \leq 4$  are shown in Fig. 14. In fact, that is the representation of the master diagram presented in Fig. 10. The pulse is stable above the corresponding curves. One may conclude that, in general case, odd higher-order dispersions destabilize a pulse so that a large positive  $\beta_2$  is required for pulse stabilization ( $\beta_2 \equiv \beta(\omega_0)$ ).

It was conjectured that a source of destabilization in this case is an excitation of dispersive waves which is caused by resonance with a continuous-wave perturbation (Kalashnikov (2011); Kalashnikov et al. (2008)). Such an excitation appears if the resonance condition is satisfied:  $k(\omega) \equiv \beta_2 \omega^2 + \sum_{n=3} \beta_n \omega^n = q$ , where  $k(\omega)$  is the wavenumber of linear wave (i.e. perturbation) and  $q$  is the wavenumber of soliton. If there is some frequency which satisfies this condition, the generation of a dispersive wave begins at the expense of a soliton that perturbs the latter.

The effect of even higher-order dispersions  $\beta_{2n}$  ( $n > 1$ ) is more complicated. If the sign of  $\beta_{2n}$  is such that the net-dispersion decreases toward the edges of soliton spectrum, the pulse can be stabilized by only larger dispersion  $\beta_2$ . For the opposite sign of  $\beta_{2n}$ , the pulse becomes stable within a wider range of dispersions and the stability border can penetrate even into anomalous dispersion region (Fig. 14).

The chirped dissipative soliton destabilized by higher-order dispersions behaves chaotically: its parameters, in particular the peak power and the central frequency, shake

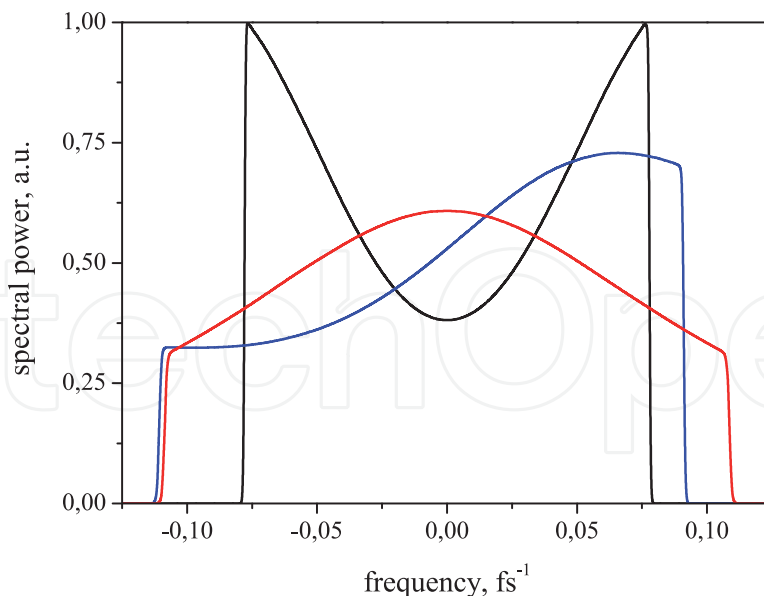


Fig. 15. Calculated spectral profiles of a Ti:sapphire oscillator for  $\beta_2 = 110 \text{ fs}^2$ ,  $\beta_4=0 \text{ fs}^4$  (red), 2000 (blue), 10000 (black),  $\beta_3=0 \text{ fs}^3$  (black, red), 300 (blue). Adapted from (Kalashnikov et al. (2005)).

(Kalashnikov et al. (2008); Sorokin et al. (2008)). This regime is called as “*chaotic mode-locking*” (Deissler & Brand (1994)) and, as a rule, separates the regimes of chirped and chirp-free pulse generation. As the extreme case, the noisy mode-locking (Horowitz et al. (1997)) can develop: pulse envelope and spectrum become completely fragmented on a small scale but preserve their localization on a large scale so that the averaged envelope and spectrum are comparatively smooth (Kalashnikov (2011); Kalashnikov et al. (2008)).

Besides an effect on the pulse stability, higher-order dispersions distort the pulse spectrum (Fig. 15). As a rule, the maximum spectral amplitude is located within a range, where the normal dispersion is larger (Kalashnikov et al. (2005)).

Also, numerical simulations have revealed that a chirped-pulse oscillator can suffer from the long-periodic pulsations (both regular and chaotic) of the pulse peak power even in the absence of higher-order dispersions (Kalashnikov & Chernykh (2007)). Such an instability growing with the dispersion was attributed to an excitation of internal perturbation modes of dissipative soliton. An important consequence of this instability is the modulation of pulse spectrum, especially, the growth of spikes at the spectrum edges (Fig. 16).

One may conclude that the numerical modeling has provided with a rich information concerning the properties of a chirped dissipative soliton: i) dependencies of main pulse parameters on the parameters of master equations have been obtained, ii) spectral profiles of chirped dissipative soliton have been classified, iii) it has been conjectured that a true parametric space of chirped-pulse oscillator has a reduced dimension, iv) pulse energy scalability has been demonstrated and concepts of “master-diagram” and “dissipative soliton resonance” have been formulated, and, at last, v) pulse stability region have been explored extensively and decisive contributions of the gain saturation and the higher-order dispersions to the pulse instability have been shown.

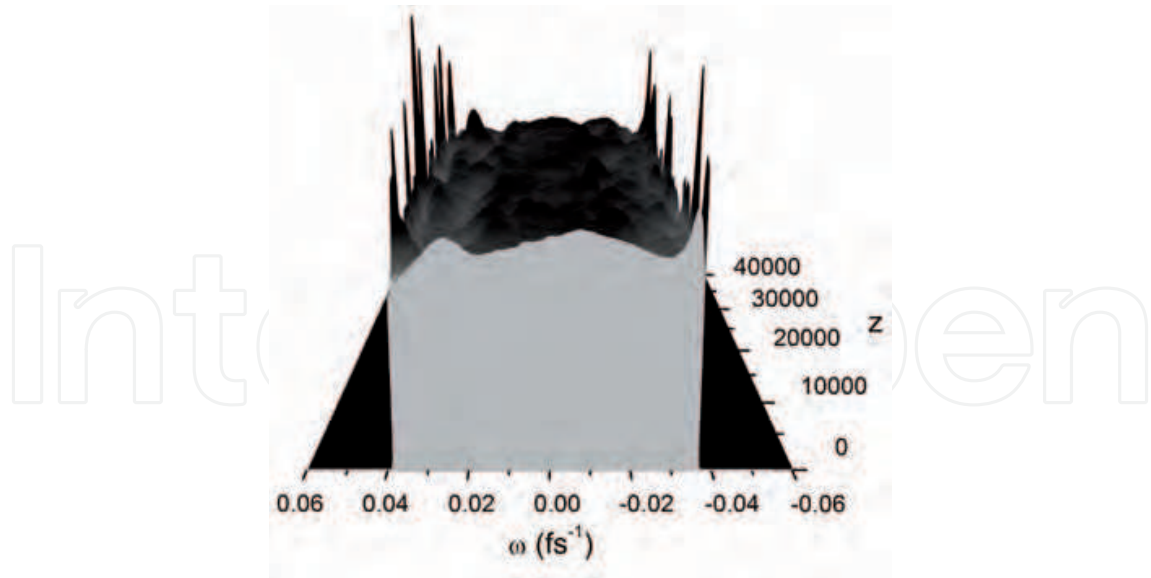


Fig. 16. Evolution of distorted spectrum profile of a Ti:sapphire oscillator,  $\beta = 150 \text{ fs}^2$ . Adapted from (Kalashnikov & Chernykh (2007)).

Nevertheless, a systematic understanding of the numerical results is hardly possible without an exploration of adequate analytical models of chirped-pulse oscillators.

### 2.3.2 Analytical models of chirped dissipative soliton

Below, basic analytical models of chirped dissipative solitons will be surveyed. For convenience, we divide these models into three groups which are based on i) exact soliton solution of the master equation, ii) solutions obtained from the adiabatic approximation, and iii) approximated solutions obtained from the variational method and the method of moments.

#### 2.3.2.1 Exact soliton solution of the CQNGLE

Eq. (17) is nonintegrable and its exact soliton solutions are known for only a few of cases, when some algebraic relations on the parameters of the equation are imposed (Akhmediev & Ankiewicz (1997)). More general solutions can be revealed on basis of the algebraic nonperturbative techniques (Conte (1999)) which, nevertheless, are not developed sufficiently still. However, a few of known exact solutions can provide with some insight into properties of a chirped-pulse oscillator.

For the CQNGLE (Eqs. (13,17)), the sole soliton solution is known (Soto-Crespo et al. (1997); van Saarloosa & Hohenberg (1992)). It can be expressed in the following form (Renninger et al. (2008))

$$A(z, \tau) = \sqrt{\frac{A}{B + \cosh(\tau/T)}} \exp \left[ -\frac{i\psi}{2} \ln(B + \cosh(\tau/T)) + iqz \right] \quad (21)$$

where  $A$ ,  $B$ ,  $T$ ,  $\psi$ , and  $q$  are the real constants characterizing pulse amplitude, shape, width, chirp, and wavenumber, respectively. It is important to emphasize, that it is a partial solution and exists for only certain algebraic relations imposed on the parameters of Eqs. (13,17).

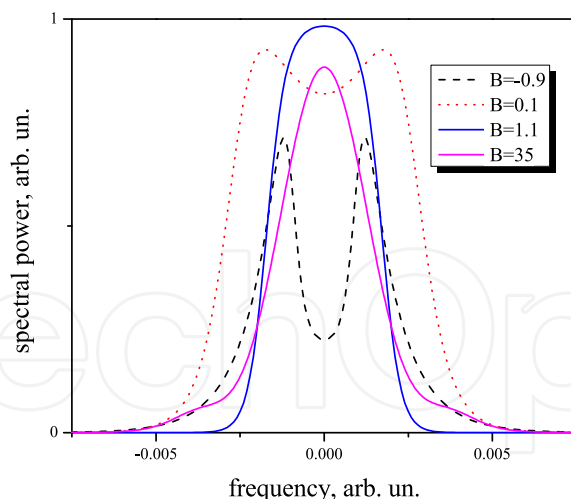


Fig. 17. Spectral profiles of a dissipative soliton (21),  $\beta/\alpha = 250$ ,  $\zeta = -0.5\gamma$  for  $B < 1$  and  $0.5\gamma$  for  $B > 1$ . The scales are arbitrary.

In spite of the fact that Eq. (21) represents only partial solution existing on some fixed hypersurface of parametrical space, it reproduces main tendencies of chirped-pulse oscillators: the energy, the chirp and the pulse duration increase with the dispersion. Also, the ratio of the self-amplitude modulation to the self-phase modulation (i.e.  $\kappa/\gamma$ ) required for (21) decreases with the growth of the ratio of the dispersion to the spectral filtering (i.e.  $\beta/\alpha$ ) (Renninger et al. (2008); Soto-Crespo et al. (1997)). The most interesting property of (21) is that it reproduces a variety of experimental and numerical spectra classified above (e.g., see Fig. 9). Examples of analytical spectra are shown in Fig. 17 in dependence on the shape parameter  $B$  (the expressions for the parameters of (21) are taken from (Renninger et al. (2008))). A steepness of spectrum edges depends on the chirp and increases with it so that the spectrum becomes truncated for  $\psi \gg 1$ .

The interesting property of solution (21) is that, even in the absence of fourth-order dispersion (Fig. 15) and perturbations (Fig. 16) it reproduces the concave spectra (black dashed curve in Fig. 17) which are often observable in an experiment. The corresponding condition is  $B < 1$  but the self-amplitude modulation is not saturable, i.e.  $\zeta < 0$ . The last condition means that the corresponding solution is unstable against a pulse collapse. It was suggested that three factors can stabilize the dissipative soliton in this case: i) gain saturation dynamics, ii) contribution of higher order terms in the self-amplitude modulation law of (13), and iii) breather-like behavior of a pulse in a real-world oscillator (Renninger et al. (2008)).

The soliton solution (21) provides with some important insights but there is some crucial disadvantage in the approach considered: in both isogain (Soto-Crespo et al. (1997)) and non-isogain (Renninger et al. (2008)) representations the exact solution imposes the strict relations on the parameters of (17). As a result, the chirped dissipative soliton can not be traced within a broad multidimensional parametrical range. Hence, the obtained picture is rather sporadic and is of interest only in the close relation with the numerical results (see above).

An additional information can be obtained on the basis of the perturbative method (Malomed & Nepomnyashchy (1990)). The important property of the corresponding solution is that it is continuously extendible to the "Schrödinger" one:  $A(z, t) \propto \cosh(t/T)^{-1+i\psi}$

when  $\zeta \rightarrow 0$  (i.e. in the absence of saturation of self-amplitude modulation). We shall call this chirped dissipative soliton as the “negative branch” one. This perturbative technique provides with a quite accurate approximation for a low-energy chirped dissipative soliton when  $\sigma\zeta/\kappa \ll 1$  (Kalashnikov (2009a)) and the corresponding parametrical range of pulse existence is  $C \leq 2 - 4\sqrt{6\sigma\zeta/5\kappa}$  ( $\sigma\zeta/\kappa \leq 1/4$ ).

As a further step in the development of analytical techniques required for the dissipative soliton exploration, two approximate methods will be considered below.

### 2.3.2.2 Adiabatic theory of chirped dissipative soliton

The adiabatic method considered in this section is developed in three main steps: i) the condition of  $T \gg \sqrt{\beta}$  allows the adiabatic approximation for Eq. (17), ii) regularization procedure is applied to the expression for the soliton frequency deviation that excludes nonphysical solutions, and iii) the method of stationary phase for the Fourier image of soliton complex envelope is applied that gives the expression for soliton spectrum and energy. The last step requires  $\psi \gg 1$ , i.e.  $\beta \gg \alpha$  and  $\gamma \gg \kappa$  (Eq. (18)).

Let's begin with the traveling wave reduction of (17):

$$A(z, \tau) = \sqrt{P(\tau)} \exp [i\phi(\tau) - iqz], \quad (22)$$

where  $P(\tau)$  is the instant power,  $\phi(\tau)$  is the phase, and  $q$  is the soliton wave-number. In the adiabatic limit  $T \gg \sqrt{\beta}$ , the substitution of (22) in the CQNGLE (13,17) results in

$$\begin{aligned} \beta\Omega(\tau)^2 &= q - \gamma P(\tau) - \chi P(\tau)^2, \\ \beta \left( \frac{\Omega(\tau)}{P(\tau)} \frac{dP(\tau)}{d\tau} + \frac{d\Omega(\tau)}{d\tau} \right) &= \kappa P(\tau) (1 - \zeta P(\tau)) - \sigma - \alpha\Omega(\tau)^2, \end{aligned} \quad (23)$$

where  $\Omega \equiv d\phi(t)/dt$  is the instant frequency.

Since  $P(\tau) \geq 0$  by definition, there is the maximum frequency deviation  $\Delta$  from the carrier frequency:  $\Delta^2 = q/\beta$ . Thus, Eqs. (23) lead, after some algebra (Kalashnikov (2009a)), to

$$\begin{aligned} \frac{d\Omega}{d\tau} &= \frac{\sigma + \alpha\Omega^2 - \frac{\kappa(Y-\gamma)}{4\chi^2} (2\chi + \zeta\gamma - \zeta Y)}{\beta [4\chi\beta\Omega^2 - (Y - \gamma) Y]} (Y - \gamma) Y, \\ Y &= \sqrt{\gamma^2 + 4\beta\chi (\Delta^2 - \Omega^2)}. \end{aligned} \quad (24)$$

The singularity points of Eq. (24) (the regularity condition is  $|d\Omega/d\tau| < \infty$ ) impose the restrictions on the  $\Delta$  value:

$$\begin{aligned} \Delta^2 &= \frac{\gamma}{16\zeta\beta \left( \frac{c}{b} + 1 \right)} \times \\ &\times \left[ \frac{2 \left( 3 + \frac{c}{b} + \frac{4}{b} \right) \left( 2 + \frac{c}{2} + \frac{3b}{2} \pm \sqrt{(C-2)^2 - 16a \left( 1 + \frac{c}{b} \right)} \right)}{1 + \frac{c}{b}} - 12 - 3c - 9b - \frac{32a}{b} \right], \end{aligned} \quad (25)$$

where three control parameters are  $a \equiv \sigma\zeta/\kappa$ ,  $b \equiv \zeta\gamma/\chi$ , and  $C \equiv \alpha\gamma/\beta\kappa$ . These three parameters define the parametric dimensionality of a chirped dissipative soliton.

In the limit of  $\chi \rightarrow 0$ , one has (Kalashnikov et al. (2006))

$$\gamma P_0 = \beta \Delta^2 = \frac{3\gamma}{4\zeta} \left( 1 - \frac{C}{2} \pm \sqrt{\left( 1 - \frac{C}{2} \right)^2 - 4a} \right), \quad (26)$$

$$\frac{d\Omega}{d\tau} = \frac{\beta\zeta\kappa}{3\gamma^2} (\Delta^2 - \Omega^2) (\Omega^2 + \Xi^2), \quad \beta\Xi^2 = \frac{\gamma}{\zeta} (1 + C) - \frac{5}{3}\gamma P_0,$$

where the equation for the peak power  $P_0$  (or, equally, for  $\Delta$ ) results from the regularity condition.

Eqs. (25,26) demonstrate two branches of soliton solutions corresponding to opposite signs before a square root. In correspondence with these two signs, the solutions will be called as “positive-branch” and “negative-branch” chirped dissipative solitons.

In the cubic nonlinear limit of Eqs. (13,20) ( $\chi \rightarrow 0$ ,  $\zeta \rightarrow 0$ ), which admits an exact chirped dissipative soliton solution (Haus et al. (1991)), one has

$$A(z, \tau) = \sqrt{P_0} \operatorname{sech} \left( \frac{\tau}{T} \right)^{1-i\psi} e^{-iqz}, \quad (27)$$

$$\alpha\Delta^2 = \frac{3\sigma C}{2-C}, \quad \gamma P_0 = \beta\Delta^2, \quad \psi = \frac{3\gamma}{\kappa(1+C)}, \quad T = \frac{3\gamma}{\kappa\Delta(1+C)}.$$

Next assumption allows a further simplification. Since the phase  $\phi(\tau)$  is a rapidly varying function due to a large chirp (the necessary requirements are  $\beta \gg \alpha$  and  $\gamma \gg \kappa$ , see Eq. (18)), one may apply the method of stationary phase to the Fourier image  $e(\omega)$  of  $A(\tau)$  (Podivilov & Kalashnikov (2005)). Then, the spectral profile corresponding to (23,24) can be written as

$$p(\omega) \equiv |e(\omega)|^2 \approx \frac{\pi(Y-1)((Y-1)Cb + 4(2\omega^2 - \Delta^2))H(\Delta^2 - \omega^2)}{CY((Y-1)(C(a+b+b^2+\omega^2) + b(\Delta^2 - \omega^2)) - 2(b+1)(\Delta^2 - \omega^2))}, \quad (28)$$

The expression for  $p(\omega)$  allows obtaining the soliton energy by integration:  $E = \int_{-\Delta}^{\Delta} \frac{d\omega}{2\pi} p(\omega)$ .

The soliton parametrical space is given by the following normalizations:  $\tau' = \tau(\kappa/\zeta)\sqrt{\kappa/\alpha\zeta}$ ,  $\Delta'^2 = \Delta^2\alpha\zeta/\kappa$ ,  $\Omega'^2 = \Omega^2\alpha\zeta/\kappa$ ,  $P' = \zeta P$ , and  $E' = E(\kappa/\gamma)\sqrt{\kappa\zeta/\alpha}$  (primes will be omitted thereafter). Hence  $Y \equiv \sqrt{1 + 4(\Delta^2 - \Omega^2)/bC}$  and  $H$  is the Heaviside's function in Eq. (28).

As it has been demonstrated in (Kalashnikov (2009a)), the truncated at  $\pm\Delta$  spectra (28) have convex, concave, and concave-convex vertexes (Fig. 18, left). When  $\chi \rightarrow 0$ , only convex truncated spectra remain (Podivilov & Kalashnikov (2005)):

$$p(\omega) \approx \frac{6\pi\gamma}{\zeta\kappa} \frac{H(\Delta^2 - \omega^2)}{\Xi^2 + \omega^2}, \quad E = \frac{6\gamma}{\kappa\zeta\Xi} \arctan \left( \frac{\Delta}{\Xi} \right). \quad (29)$$

At last, for the cubic nonlinear limit of Eq. (13,20) ( $\chi \rightarrow 0$ ,  $\zeta \rightarrow 0$ ) one may obtain (Kalashnikov (2009b))

$$p(\omega) \approx \frac{6\pi\beta}{\kappa(1+C)} H(\Delta^2 - \omega^2), \quad E = \frac{6\beta\Delta}{(1+C)\kappa}. \quad (30)$$

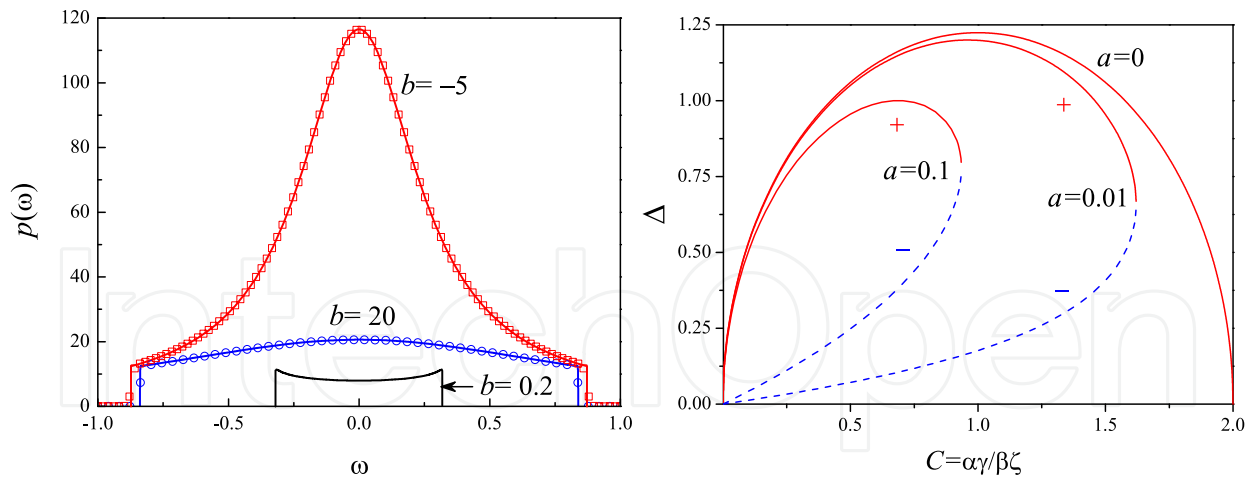


Fig. 18. Left: Spectra corresponding to the positive-branch (i.e. + sign in Eqs. (25,26)) of chirped dissipative soliton for  $C = 1$ ,  $a = 0.01$  and different values of  $b$ .  $b > 0$  corresponds to an enhancement of the self-phase modulation with the power growth and  $|b| \rightarrow \infty$  corresponds to an absence of the quintic self-phase modulation, i.e.  $|\chi| \rightarrow 0$ . Squares and circles represent the numerical spectral profiles. Adapted from (Kalashnikov (2009a)). Right: Normalized spectral half-widths in dependence on  $C$  for the different values of  $a$  ( $\chi = 0$ ). Positive branch - red solid curves, negative branch - dashed blue curves. Adapted from (Kalashnikov (2009b)).

That is the truncated flat-top spectrum, which approximates the spectrum of exact solution of the cubic nonlinear complex Ginzburg-Landau equation.

The important property of the integration procedure considered is that it is applicable to various types of self-amplitude modulation. For instance, one has for Eqs. (14,20) (Kalashnikov (2009b); Kalashnikov & Apolonski (2009)):

$$\begin{aligned} \kappa P_0 &= \frac{\alpha}{\ell' C} \Delta^2 = \frac{3}{4C} \left[ 2(1 - \zeta) - C \pm \sqrt{Y} \right], \\ \frac{d\Omega}{d\tau} &= \frac{\alpha}{3\beta} \frac{(\Delta^2 - \Omega^2)(\Xi^2 - \Omega^2)}{\Delta^2 - \Omega^2 + \gamma/\kappa\beta}, \quad \frac{\alpha}{\ell'} \Xi^2 = \frac{2\alpha}{3\ell'} \Delta^2 + 1 - \zeta + C, \\ p(\omega) &\approx \frac{6\pi\beta^2}{\alpha\gamma} \frac{\Delta^2 - \omega^2 + \gamma/\kappa\beta}{\Xi^2 - \omega^2} \text{H}(\Delta^2 - \omega^2), \end{aligned} \quad (31)$$

where  $\zeta \equiv \sigma/\ell'$ , and  $Y \equiv (2 - C)^2 - 4\zeta(2 - \zeta + C)$ . For the above introduced normalizations with the replacement of  $\zeta$  by  $\kappa$ , the dimensionless energy is

$$E = \frac{6\Delta}{C^2} \left[ 1 - \frac{(\Xi^2 - \Delta^2 - C) \operatorname{arctanh}\left(\frac{\Delta}{\Xi}\right)}{\Delta\Xi} \right]. \quad (32)$$

It should be noted, that the presented technique based on the adiabatic approximation and the regularization of  $d\Omega/dt$  is analogous to that of (Ablowitz & Horikis (2009)). However, an approximate integration in the spectral domain allows us the further reduction of parametric space dimension and the construction of physically meaningful master diagrams that makes the soliton properties to be easily traceable.

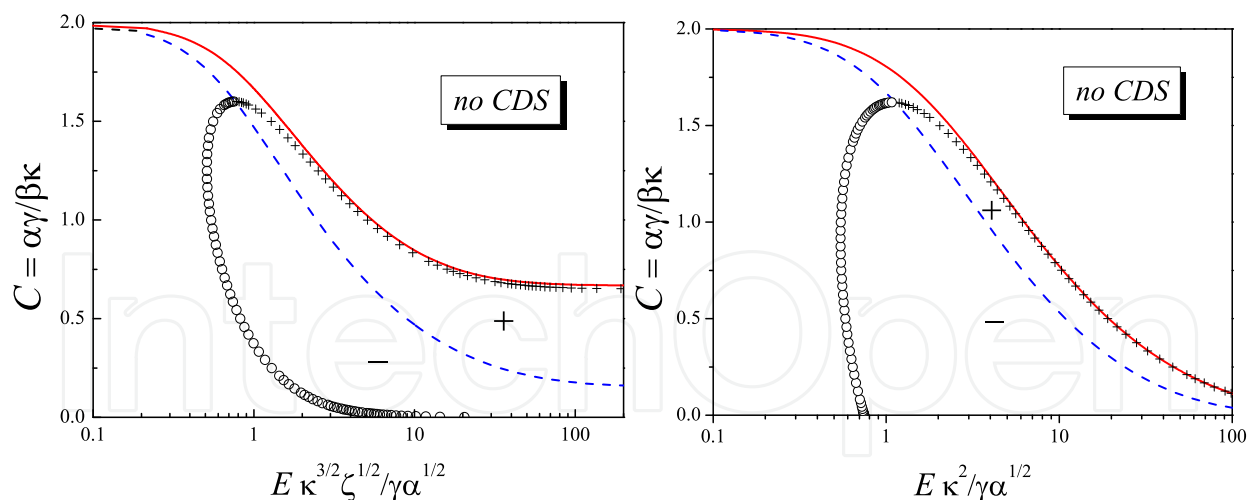


Fig. 19. Left: master diagram for the chirped dissipative soliton (CDS) of Eqs. (13,17),  $\chi = 0$ . There exists no soliton above the red curve (therein  $\sigma < 0$ , i.e. the vacuum of (17) is unstable).  $a = 0$  (zero-level isogain) along the red curve. Blue dashed curve divides the regions, where the positive (+) and negative (-) branches of (25,26) exist. Crosses (circles) correspond to the +(-) branch for  $a=0.01$ . The normalization for energy is restored. Adapted from (Kalashnikov (2009a)). Right: master diagram for the chirped dissipative solitons corresponding to Eqs. (31,32). Red curve is the stability threshold ( $\zeta = 0$ ), blue curve divides the regions of positive and negative branches which are shown for  $\zeta = 0.01$  by crosses and circles, respectively. Adapted from (Kalashnikov (2009b)).

A *master diagram* connects the normalized energy with the parameter  $C$  along an isogain. The example of master diagram for the CQNGLE with vanishing quintic self-phase modulation (i.e.  $\chi \rightarrow 0$  in (15)) is presented in Fig. 19 (left). The chirped dissipative soliton has a two-dimensional parametric space in this case. The solid red curve  $a = 0$  shows the border of the soliton existence. Above this border, the vacuum of Eq. (20) is unstable. One may see that the stability threshold on  $C$  decreases with  $E$ . Physically, that means, for instance, the dispersion growth and the self-phase modulation reduction required for obtaining the more energetic pulses. The blue dashed curve divides the existence regions for the positive and negative branches of soliton (the corresponding signs in Eq. (25,26)). The branches merge along this curve. Crosses (circles) represent the curve along which there exists the positive (negative) branch for some fixed value of  $a$  (*isogain curve*).

The master diagram reveals four significant differences between the positive and negative branches of chirped dissipative soliton. The first one is that the negative branch has lower energy than the positive one for a fixed  $C$ . The second difference is that the positive branch has a finite limit on  $C$  for  $E \rightarrow \infty$ . For the zero-level isogain such a limit is  $C \approx 0.66$  in the case considered. This value decreases with  $\chi > 0$  and increases with  $\chi < 0$ . The existence of such “resonant”  $C$  allows concluding that the positive branch is energy scalable. This means that the soliton energy growth does not require a substantial change of  $C$ , i.e. the change of relation between spectral dissipation and self-phase modulation from one side and dispersion and self-amplitude modulation from another side. Such a property corresponds to the notion of the dissipative soliton resonance of (Grelu et al. (2010)). In the terms of (Kalashnikov et al. (2006)), the resonant dissipative soliton is an overdeveloped soliton with

the finger-like spectrum ( $\Delta \gg \Xi$  in (29)) that is the pulse with the almost Lorentz spectrum and the truncated flat-top temporal profile.

The negative branch is not energy scalable, that is the energy growth along this branch needs a substantial decrease of  $C$  (e.g., owing to a dispersion growth or a self-phase modulation reduction). The third difference is that the positive branch verges on  $a=0$  within a whole range of  $E$ . The fourth difference is that the negative branch has a Schrödinger soliton limit (27) for  $\zeta, \chi \rightarrow 0$  (Eq. (13,17)). The detailed description of master diagrams, pulse characteristics, spectra and temporal profiles of chirped dissipative solitons in the presence of quintic self-phase modulation  $\chi \neq 0$  can be found in (Kalashnikov (2009a)).

It is of interest to compare the master diagrams for the chirped dissipative solitons of the CQNGLE (13,17) and the complex nonlinear Ginzburg-Landau equation with a perfectly saturable absorber (14,17) (see (31,32)). Master diagram for the latter is shown in Fig. 19 (right). Its structure is similar to that in Fig. 19 (left) but there exist two important differences. First, the  $C$ -parameter tends asymptotically to zero with the energy growth. This means that there is no dissipative soliton resonance in this case. Secondly, the energy on an isogain for the negative soliton branch remains almost constant with  $C \rightarrow 0$ . One may call this phenomena as the dissipative soliton antiresonance. Nevertheless, in spite of absence of perfect energy scalability (i.e. absence of the dissipative soliton resonance), the energy of positive soliton branch can be scaled with  $C$  in agreement with the following approximate asymptotical law:

$$E \approx \frac{18\ell' \beta^2}{\gamma \alpha^{3/2}}. \quad (33)$$

This scaling law assumes  $C \ll 1$  and gives the energy at the zero-level isogain  $\zeta = 0$ , i.e. at the stability threshold. The quadratic dependence of energy on dispersion is very promising because comparatively moderate dispersions can provide high energies. Also, it is very important that the energy is proportional to the cube of a gain bandwidth that offers advantages to the broadband active media. In agreement with Eq. (33), approximately linear energy growth with the modulation depth as well as faster than linear energy growth with the spectral filter bandwidth have been demonstrated experimentally for a dissipative soliton fiber laser (Lecaplain et al. (2011)).

The spectral width of the dissipative soliton is of interest because it defines the pulse width after extra-resonator compression:  $T \approx 2/\Delta$ . For the negative branch having narrower spectrum than the positive branch, the spectral width decreases with the  $C$ -decrease (Fig. 18, right) owing to the dispersion growth ( $C \propto 1/\beta$ ) which stretches the pulse when the energy remains almost constant (compare with (Chong et al. (2008b))). When the energy  $E$  changes weakly along an isogain corresponding to the negative branch, the spectrum broadens with the  $\alpha$ -increase ( $C \propto \alpha$ ), i.e. the gainband narrowing (Fig. 18, right). The explanation is that the growth of spectral filtering enhances a cut-off of spectral components located on the pulse edges (Fig. 6, right). As a result, the pulse shortens and, for a fixed energy, the peak power  $P_0$  increases. Since  $\Delta^2 \propto P_0$  (Eqs. (26,27,31)), the spectrum broadens. For the positive branch, the spectrum initially broadens with the  $C$ -decrease (Fig. 18, right) because the energy  $E$  and, consequently, the self-phase modulation grow along an isogain (Fig. 19). However, further decrease of  $C$  narrows the spectrum like the negative branch in agreement with the numerical results of (Siegel et al. (2008)). It is important to note that the dependence of  $\sigma$  on the energy for a fixed  $C$  is inverse for the negative and positive branches:  $\sigma$  increases with  $E$  for the former and decreases for the latter. Hence, Fig. 18 (right) allows concluding that the spectrum

broadens with energy (up to some  $\Delta = \text{const}$  for the positive branch). Such a result has been corroborated by the numerical simulations (Siegel et al. (2008)).

Another important characteristic of chirped dissipative soliton is its chirp, which has to be  $\gg 1$  to provide the energy scalability. The chirp at the pulse center (where  $\tau = 0$  by definition) normalized to  $\kappa/\zeta\beta$  is (Kalashnikov (2009a))

$$\psi|_{\tau=0} \equiv \left. \frac{d\Omega}{d\tau} \right|_{\Omega=0} = -a - \frac{b^2}{4} (1 - Y|_{\Omega=0}) \left( 1 + \frac{2}{b} - Y|_{\Omega=0} \right), \quad (34)$$

where  $Y = \sqrt{1 + 4(\Delta^2 - \Omega^2)/cb}$  is the normalized version of the corresponding expression from (24). For a soliton solution (i.e. an isolated solution with the appropriate asymptotic  $\lim_{\tau \rightarrow \pm\infty} P(\tau) = 0$ ), the chirp has to be positive that agrees in the limits of  $\beta/\alpha \gg 1$  and  $\gamma/\kappa \gg 1$  with the analytical theory presented in (Soto-Crespo et al. (1997)) where  $0 < \psi \approx 3\gamma/(1+C)\kappa < \beta/\alpha$  (here  $\psi$  is defined as the parameter in the phase profile ansatz  $\phi(\tau) \equiv \psi \ln \sqrt{P(\tau)}$ ). It is interesting that the positive (i.e. energy scalable) soliton branch disappears when the self-phase modulation saturation is strong:  $0 > b \geq -2$ . In this case, the “antisoliton” appears which has a truncated (i.e.  $\lim_{\tau \rightarrow T} P(\tau) = 0$ ) parabolic-top temporal profile with  $\lim_{\tau \rightarrow T} \Omega(\tau) = \pm\infty$  (Kalashnikov (2009a)). Formally, such a soliton has the temporal and spectral shapes exchanged in comparison with those for an ordinary chirped dissipative soliton. Such an “antisoliton” has been observed in (Liu (2010)) and possesses an enhanced energy scalability.

One may conclude that the adiabatic theory of chirped dissipative solitons provides with a deep insight into physics of chirped-pulse oscillators. The pulse characteristics become easily traceable and finding of the true parametrical space of soliton allows looking at an extremely broad range of oscillators from a unified point of view. Nevertheless, the underlying approximations of: i) strong domination of the nondissipative effects (dispersion and self-phase modulation) over the dissipative ones (spectral filtering and self-amplitude modulation), ii) negligible contribution of the higher-order dispersions, and iii) distributed character of a laser system impose some restrictions. Second approximation is sound for the thin-disk oscillators based on comparatively narrow-band active media like Yb:YAG. The last approximation is well-grounded for the high-energy solid-state oscillators in general. Moreover, the simple analytical expressions for the complex spectral amplitude of soliton allow developing the perturbation theory in spectral domain (e.g., see (Kalashnikov (2010; 2011); Kalashnikov et al. (2011))). Nevertheless, another analytical approaches can shed light on some properties of chirped-pulse oscillators which are beyond the scope of the adiabatic theory.

### 2.3.2.3 Truncation of phase space: variational approximation and method of moments

Both variational approximation and method of moments allow truncating the space of (unknown) solutions of (17) to a sub-space of soliton-like ones by some appropriate ansatz (for an overview see (Anderson et al. (2001); Ankiewicz et al. (2007); Malomed (2002); Perez-Garcia et al. (2007))). The ansatz, as a rule, is the known analytical solution (21) or its reduced representation. As a result, the complex dynamics of (17) becomes to be reduced to the comparatively simple one described by a set of ordinary differential equations governing

an evolution of the ansatz parameters (pulse amplitude, width, chirp, etc.). As a result, the problem becomes semi-analytical (Tsoy et al. (2006); Usechak & Agrawal (2005)).

The variational approximation can be sketched in the following way. The factors governing the pulse dynamics are divided into two parts: dissipative and nondissipative ones. The last underlying the nonlinear Schrödinger equation (Eqs. (15,16)) can be described by the Lagrangian. In absence of higher-order dispersions and quintic self-phase modulation, the corresponding Lagrangian density is

$$\mathcal{L} = \frac{i}{2} \left[ A^*(z, \tau) \frac{\partial A(z, \tau)}{\partial \tau} - A(z, \tau) \frac{\partial A^*(z, \tau)}{\partial \tau} \right] - \frac{\beta}{2} \frac{\partial A(z, \tau)}{\partial \tau} \frac{\partial A^*(z, \tau)}{\partial \tau} + \frac{\gamma}{2} |A(z, \tau)|^2. \quad (35)$$

Eq. (35) defines the nonlinear Schrödinger equation through the Lagrange-Euler equation. The dissipative part of the CQNGLE (see Eqs. (13,20)) is described by the driving force:

$$\mathcal{Q} = -i\sigma A(z, \tau) + \frac{ig_0}{1 + E_s^{-1} \int_{-\infty}^{\infty} |A|^2 d\tau'} \left[ A(z, \tau) + \tau \frac{\partial^2}{\partial \tau^2} A(z, \tau) \right] + ik \left[ |A(z, \tau)|^2 - \zeta |A(z, \tau)|^4 \right] A(z, \tau). \quad (36)$$

The force-driven Lagrange-Euler equations

$$\frac{\partial \int_{-\infty}^{\infty} \mathcal{L} d\tau}{\partial \mathbf{f}} - \frac{\partial}{\partial z} \frac{\partial \int_{-\infty}^{\infty} \mathcal{L} d\tau}{\partial \mathbf{f}} = 2\Re \int_{-\infty}^{\infty} \mathcal{Q} \frac{\partial A^*}{\partial \mathbf{f}} d\tau \quad (37)$$

allow obtaining a set of the ordinary first-order differential equations for a set  $\mathbf{f}$  of the soliton parameters if one assumes the soliton shape in the form of some trial function  $A(z, \tau) \approx \mathcal{F}[\mathbf{f}(z, \tau)]$ . One may chose (Kalashnikov & Apolonski (2010))

$$\mathcal{F} = A_0(z) \operatorname{sech} \left( \frac{\tau}{T(z)} \right) \exp \left[ i \left( \phi(z) + \psi(z) \ln \left( \operatorname{sech} \left( \frac{\tau}{T(z)} \right) \right) \right) \right], \quad (38)$$

with  $\mathbf{f} = \{A_0(z), T(z), \phi(z), \psi(z)\}$  describing amplitude, width, phase, and chirp of dissipative soliton, respectively.

Substitution of (38) into (37) results in four equations for the soliton parameters. These equations are completely solvable for a steady-state propagation (i.e. when  $\partial_z A_0 = \partial_z T = \partial_z \psi = 0$ , but  $\partial_z \phi \neq 0$ ).

As it taken a place in the adiabatic theory (see Fig. 19, left), the dissipative soliton is completely characterized by two-dimensional master diagram if  $C \ll 1$  (Fig. 20, left). The red curve in Fig. 20 corresponds to the stability threshold obtained from the adiabatic theory (see Eq. (29)): the soliton is unstable on the right of this curve. The positive branch solution with convex spectrum, which is predicted by the adiabatic theory, cannot be obtained from the Schrödinger-like ansatz (38) so that the solution for the latter is situated on the left of the curves corresponding to the different values of  $\gamma/\kappa$  shown in Fig. (20). These curves are the zero-level isogains for pulses (38). One has note, that the requirement of  $\gamma \gg \kappa$  is not essential for the variational approximation. Nevertheless, one may see that all solutions have a single asymptotic (dashed curve) for  $C \ll 1$  so that the master diagram is two-dimensional

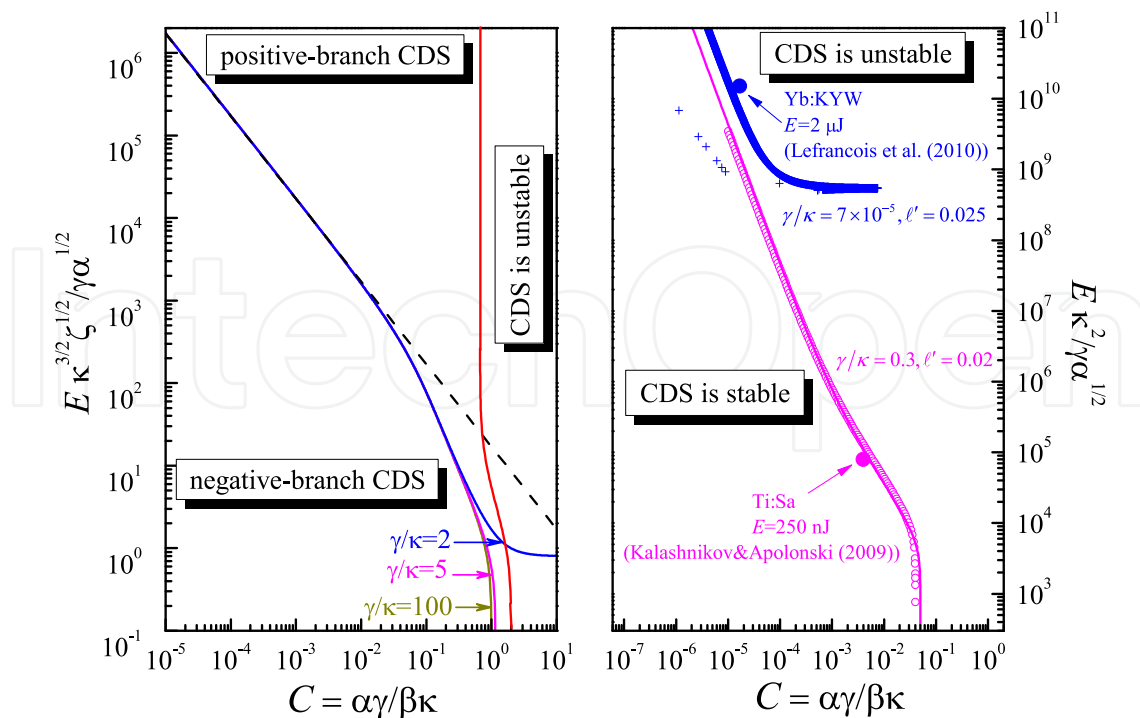


Fig. 20. Left: master diagram of a chirped dissipative soliton (CDS) for the self-amplitude modulation (13) (CQNGLE). The red solid curve corresponds to the stability threshold obtained from the adiabatic approximation (29). Another colored curves correspond to the thresholds obtained from the variational approximations with the ansatz (38) for the different values of  $\gamma/\kappa$ . The dashed line corresponds to the asymptotic  $C \ll 1$ . Right: analogous master diagram for the self-amplitude modulation (14). Crosses and circles show the stability thresholds for a chirped dissipative soliton (CDS) obtained from the variational approximation. The solid line corresponds to the adiabatic approximation with  $\ell' = 0.02$ . The parameters are shown in Figure. Points correspond to the experimental operational points of two solid-state oscillators. Right figure is adapted from (Kalashnikov & Apolonski (2010)).

(i.e. it does not depend on the  $\gamma/\kappa$ -value) in this limit. The asymptotical values of the pulse parameters along the dashed curve are:

$$E \approx \frac{17\beta}{\sqrt{\alpha\kappa\zeta}}, \quad T \approx \frac{8}{C} \frac{\gamma}{\kappa} \sqrt{\frac{\alpha\zeta}{\kappa}}. \tag{39}$$

The importance of these scaling rules (compare with Eq. (33)) is that they correspond to the flat-top spectrum relevant to (38), which has the spectral chirp with a weak frequency-dependence within the range of  $[-\Delta, \Delta]$  (Podivilov & Kalashnikov (2005)). As a result, such a pulse is almost perfectly compressible that is the energy loss due to satellite generation in the process of compression is minimal.

In the case of self-amplitude modulation defined by (14), the master diagram obtained with the help of the variational approximation and the ansatz (38) is shown in Fig. 20, right. Crosses and circles correspond to the stability thresholds (zero-level isogain) dictated by the variational approximation and correspond to the parameters shown in Figure. The solid curve is based on the adiabatic theory (see Eqs. (31,32)). The points correspond to the operational

points of two different oscillators (bulk and thin-disk solid-state ones). The asymptotical energy scaling law is matched perfectly by Eq. (33).

Two observations are of interest. Firstly, the asymptotical scaling law is valid for the systems with the extremely different ratio  $\gamma/\kappa$  (e.g., for a thin-disk oscillator with suppressed self-phase modulation and a Ti:sapphire oscillator with a comparatively large nonlinear phase shift). This means that a true parametrical space of chirped dissipative soliton remains two-dimensional. Secondly, the ansatz (38) covers the space of adiabatic solutions better than it takes a place in the case of CQNGLE (compare Figs. 20 left and right). The last results from the difference of spectral profiles of (31) and (29). The former corresponding to the self-amplitude modulation (14) has not finger-like profiles and is nearer to a flat-top spectrum of (38).

More general ansatz (21) allows describing a variety of spectra appearing in the normal dispersion regime (Bale & Kutz (2008)) and, that is especially important, one may simulate an unsteady pulse dynamics in both distributed (Ankiewicz et al. (2007)) and undistributed (Bale & Kutz (2008)) laser systems. In comparison with the full-sized simulations based on Eq. (20), the truncation of phase space reduces the problem of pulse dynamics to the solution of a set of nonlinear ordinary first-order differential equations for the pulse parameters ( $\partial_z \mathbf{f} \neq 0$  in Eq. (37) in this case). As a result, the task of optimization of undistributed oscillator can be solved and, for instance, the optimal placement of laser elements and the optimal dispersion map parameter can be defined (Bale et al. (2010; 2009; 2008b)). Also, an important advantage of the approach considered is that it allows investigating the dynamic stability of soliton solutions like (21,38) (e.g., see (Bale et al. (2008a))). However, it is important to remember that the results obtained on the basis of simulations in a truncated phase space require verification by full-sized simulations of Eqs. (17) or (20).

The method of moments (Maimistov (1993); Perez-Garcia et al. (2007)) is akin to the variational one. It considers a set of moments of the nonlinear Schrödinger equation (which consists of nondissipative terms of Eq. (17) and omits higher-order dispersions, quintic self-phase modulation, etc.) with the subsequent study of their evolution under action of the dissipative terms, higher-order phase nonlinearity, higher-order dispersions, etc. For instance, the first five moments are (Chang et al. (2008b); Maimistov (1993))

$$\begin{aligned} E &= \int_{-\infty}^{\infty} |A|^2 d\tau, \quad P = \int_{-\infty}^{\infty} \left( A \frac{\partial A^*}{\partial \tau} - A^* \frac{\partial A}{\partial \tau} \right) d\tau, \quad I_1 = \int_{-\infty}^{\infty} \tau |A|^2 d\tau, \\ I_2 &= \int_{-\infty}^{\infty} \tau^2 |A|^2 d\tau, \quad I_3 = \int_{-\infty}^{\infty} \tau \left( A \frac{\partial A^*}{\partial \tau} - A^* \frac{\partial A}{\partial \tau} \right) d\tau, \quad \text{etc.} \end{aligned} \quad (40)$$

Here first two moments are the energy  $E$  and the momentum  $P$ . If one denotes all dissipative terms as well as higher-order dispersions and phase nonlinearities as  $R[A]$ , the evolution of moments can be described in the following way:

$$\begin{aligned} \frac{dE}{dz} &= i \int_{-\infty}^{\infty} (AR^* - A^*R) d\tau, \quad \frac{dP}{dz} = -i \int_{-\infty}^{\infty} \left( \frac{\partial A}{\partial \tau} R^* - \frac{\partial A^*}{\partial \tau} R \right) d\tau, \\ \frac{dI_1}{dz} &= -2i\beta P + i \int_{-\infty}^{\infty} \tau (AR^* - A^*R) d\tau, \quad \frac{dI_2}{dz} = 2i\beta I_3 + i \int_{-\infty}^{\infty} \tau^2 (AR^* - A^*R) d\tau, \\ \frac{dI_3}{dz} &= -i \int_{-\infty}^{\infty} \left( 4\beta \left| \frac{\partial A}{\partial \tau} \right|^2 + \gamma |A|^4 \right) d\tau + 2i \int_{-\infty}^{\infty} \tau \left( \frac{\partial A}{\partial \tau} R^* - \frac{\partial A^*}{\partial \tau} R \right) d\tau - i \int_{-\infty}^{\infty} (AR^* - A^*R) d\tau. \end{aligned} \quad (41)$$

The system (41) is exact and the next step is analogous to that for the variational approximation: we truncate the phase space by substitution of a trial function in place of  $A$ . As a result, one has a set of nonlinear ordinary first-order differential equations for evolvable pulse parameters which allows exploring the pulse dynamics and stability like the variational approach (e.g., see (Tsoy & Akhmediev (2005); Tsoy et al. (2006); Usechak & Agrawal (2005))).

The most impressive result of the method of moments concerning the theory of chirped-pulse oscillators is conception of the so-called dissipative soliton resonance which is a representation of master diagram asymptotic  $E \rightarrow \infty$  (see Sec. 2.3.2.2). The corresponding approximate condition is (Chang et al. (2008b)):

$$\left(6.333 + \frac{3.8}{b}\right) C = 2, \quad (42)$$

where the normalizations of (25) are used.

Eq. (42) gives approximately two-fold deviation from the results of the numerical simulations (see dashed curve in Fig. 11 and (Chang et al. (2009))) and the adiabatic theory (Kalashnikov (2009a)) but, nevertheless, it provides with the correct representation of soliton parametric space and the tendencies of its asymptotic behavior. In particular, the constant spectral width is predicted in the limit of  $E \rightarrow \infty$  when  $C \rightarrow const$  in agreement with the adiabatic theory (see Fig. 18 (right), positive branch with  $C = const$  and decreasing  $a$ ; and Figs. 19). Since  $\Delta \rightarrow const$ , the peak power  $P_0$  remains constant, as well (Eq. (26)). Hence, the energy scaling is provided by scaling of the pulse width.

One may conclude that the phase space truncation methods have allowed obtaining the correct asymptotic representation of the parametric space of chirped dissipative soliton and revealing the structure of this space in agreement with the results of both numerical simulations and adiabatic theory. As a result, a unified point of view on a variety of chirped-pulse oscillators becomes possible. Moreover, the advantages of the truncation methods are that they allow exploring the unsteady pulse evolution as well as the undistributed laser systems. Another important advantage of these methods is that they permit to widen the dimensionality of Eqs. (17,20) by including the transverse spatial dimensions and to consider a space-time dynamics of an oscillator. Some partial reductions of the space-time dynamics have been used in the numerical simulations (e.g., (Kalosha et al. (1998))) and semi-analytical matrix formalism has been developed (Jirauschek & Kärtner (2006); Kalashnikov (2003)). Nevertheless, the space-time theory of chirped pulse oscillators is not developed to date.

### 3. Experimental realizations of solid-state chirped-pulse oscillators

In this part, some experimental realizations of chirped-pulse oscillators will be considered. Although the theory of chirped dissipative soliton is suitable for both solid-state and fiber lasers, we confine ourselves exclusively to the former. Also, the energy scalable solid-state oscillators operating in the anomalous (i.e. negative in our terms) dispersion regime (Steinmeyer et al. (1999); Südmeyer et al. (2008)) are beyond the scope of this review. Taking into account these limitations, one may divide the oscillators considered into two classes different by an active medium thickness, diode-pump ability and average power scalability: i) bulk and ii) thin-disk oscillators. The last class possesses excellent average power scaling properties and diode-pump ability (Giessen & Speiser (2007)) but the available active media

have comparatively narrow gainbands (i.e. the large  $\alpha$ -parameter in Eq. (19)). The bulk crystalline media, vice-versa, have limitations of power scaling but, as a rule, are broadband (Sorokina (2003)). Of course, such a division is not fundamental and the thin-disk laser systems evolve in a direction of broader available gainbands (Südmeyer et al. (2009)).

The femtosecond pulse breakthrough for a Ti:sapphire oscillator has been closely connected with the dispersion compensation technique (Spence & Sibbett (1991)). As a result, the first normal (i.e. positive) dispersion regime in this broadband mode-locked oscillator has been observed and characterized immediately (Proctor et al. (1993)). The regime obtained has demonstrated the truncated spectra of chirped picosecond pulses. It was observed that this regime is disconnected from the anomalous dispersion one due to instability in the vicinity of zero dispersion. The connection with the theoretical model of (Haus et al. (1991)), where the mechanism of chirped-pulse formation has been suggested, has been declared. The next step was an observation that a chirped-pulse oscillator allows the pulse energy scaling (Apolonski et al. (2000); Fernandez et al. (2004)). The result was a swift rise of the pulse energy from a Ti:sapphire chirped-pulse oscillator (Fernández et al. (2007); Naumov et al. (2005); Siegel et al. (2009)). The decisive steps were the cavity period  $T_{rep}$  growth and the positive dispersion control within a broad spectral range (Pervak et al. (2008)). The results are shown in Fig. 21. The near-1- $\mu$ J pulses with a compressibility down to sub-40 fs have been obtained. The preferable mode-locking technique for a highest-energy pulse generation in the case of a reduced oscillator repetition-rate is based on a semiconductor saturable absorber (Kalashnikov et al. (2006); compare Eqs. (33,39) where the scaling law is more promising for a perfectly saturable absorber). A further pulse energy growth by the means of a growth of cavity period is problematical because the gain relaxation time of 3  $\mu$ s for this medium is about of an ultimate  $T_{rep}$  and the gain dynamics begins to destabilize the pulse (Kalashnikov et al. (2006)).

As a development of the chirped-pulse oscillator technique, a further shift into the infrared generation range taken a place (Cankaya et al. (2011); Lin (2010); Sorokin et al. (2008); Tan et al. (2011)). The characteristics of a Cr:forsterite broadband oscillator approach the Ti:sapphire ones (Cankaya et al. (2011)). The problem is that the relative contribution of higher-order dispersions increases in the mid-infrared range. As a result, the pulse spectra becomes distorted and the chaotic mode-locking becomes the principal destabilizing mechanism (Kalashnikov et al. (2011); Sorokin et al. (2008)). Nevertheless, the potential of such media as Cr-doped chalcogenides allows reaching around-1- $\mu$ J sub-100 fs pulses at 2.5  $\mu$ m wavelength.

The technique of averaged power scaling based on using the thin-disk diode-pumped media (Giessen & Speiser (2007)) has allowed reaching a highest sub-picosecond pulse energies in the anomalous (negative) dispersion regime (Südmeyer et al. (2008)). In such a regime the scaling law obtained from the variational approximation for a perfectly saturable absorber is

$$E \propto \frac{|\beta|}{\gamma\sqrt{\alpha}} \quad (43)$$

and the comparison with Eq. (33) shows that the dispersion required for a pulse stabilization in a chirped-pulse oscillator can be substantially lower. Such a conclusion is supported by data of (Palmer et al. (2008; 2010)) where the high-energy pulses of approximately 400 fs width are realized by using a moderate positive dispersion (750 fs<sup>2</sup> and ranging from 1500 to 4700 fs<sup>2</sup> for different configurations) for the pulse stabilization. Another advantage of

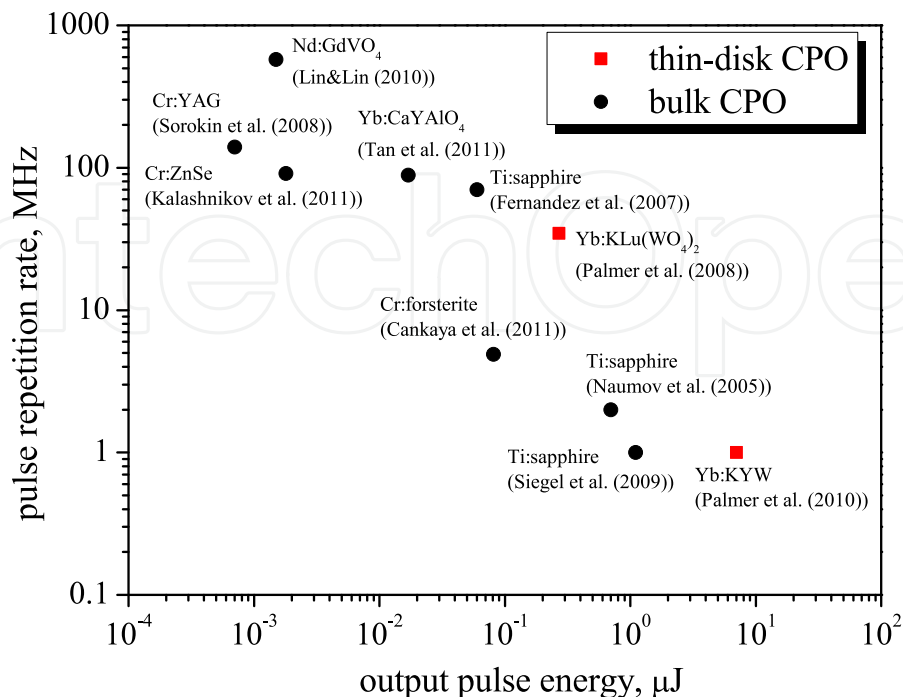


Fig. 21. Experimental realizations of chirped-pulse solid-state oscillators.

the positive dispersion regime over the negative one is the cubic energy scaling with a gain bandwidth versus the linear one for the latter (Eqs. (33,43)). Therefore, the use of more broadband materials like Yb:Lu<sub>2</sub>O<sub>3</sub>, Yb:LuScO<sub>3</sub>, and Yb:CALGO (Südmeyer et al. (2009)) is very promising for a further energy scaling in the positive dispersion regime.

One may conclude that the experimental realization of chirped-pulse oscillators is at the beginning of the development. Although the scaling potential of Ti:sapphire, it seems, is close to exhaustion, the mid-infrared broadband media like Cr:ZnSe and Cr:ZnS are extremely promising for a further development which can be achieved by enhancement of pumping sources and chirped mirrors. On the other hand, a swift growth of pulse energy of thin-disk oscillators is expected. As the numerical simulations have demonstrated (Kalashnikov & Apolonski (2010)), the pulses with 100  $\mu\text{J}$  energies are completely accessible in a thin-disk chirped-pulse oscillator with perfectly saturable absorber (see scaling rule (33)). A further progress will be based on an optimization of oscillator, SESAM and pump designs; on a progress in the chirped mirror technology; on using the more broadband active media and, probably, on a transition to the Kerr-lens mode-locking technique.

#### 4. Conclusion

A rapid progress in the field of energy scaling of femtosecond pulse oscillators has yielded three main fruits: i) thin-disk solid-state oscillators operating in the anomalous-dispersion regime, ii) both bulk and thin-disk oscillators operating in the normal dispersion regime, and iii) fiber lasers operating in the net-normal dispersion regime. In this review, the second type of oscillators has been under consideration. It was affirmed, that the source of energy scalability is a formation of chirped dissipative soliton therefore these oscillators are named

“chirped-pulse oscillators”. The main factors governing the chirped dissipative soliton have been considered and the decisive contribution of dissipative effects such as saturable gain, spectral filtering and self-amplitude modulation has been analyzed.

The theory of such solitons demonstrates that the relevant control parameters for a chirped dissipative soliton are some specific dimensionless combinations of oscillator parameters but not their absolute values. As a result, a chirped dissipative soliton “lives” in a low-dimensional parametric space and a variety of chirped-pulse oscillators (including the fiber ones) can be considered from a unified point of view. The insight into nature of dissipative soliton parametric space underlies the interrelated concepts of “master diagram” and “dissipative soliton resonance”. The achievement of these concepts is the formulation of extremely simple scaling rules which relate the pulse parameters with those of an oscillator. As a result, the properties of chirped-pulse oscillator becomes to be easily traceable within an extremely broad parametric range. Also, these rules allow comparing between different mode-locking mechanisms and demonstrate the advantage of the normal dispersion regime over the anomalous dispersion one in further energy scaling.

The stability of chirped-pulse oscillators has been considered with respect to gain saturation, higher-order dispersions and internal spectral perturbations. The numerical simulations demonstrate a variety of destabilization scenarios including the chaotic mode-locking induced by the odd-order dispersions and by the dispersion decrease towards the pulse spectrum edges. It was conjectured that the underlying mechanism is a resonance with dispersive waves but the corresponding analytical theory remains to be undeveloped, to date. The noise properties and the self-starting ability of mode-locking in the positive dispersion regime remain to be controversial, as well.

The experimental realizations of chirped-pulse solid-state oscillators have been surveyed. For convenience, the oscillators have been divided into bulk and thin-disk ones. At this moment, the bulk active media are more broadband than the thin-disk ones. There are another differences (gain relaxation times, thermal properties, diode-pump abilities, etc.), as well. But it is clear at this moment, that the chirped-pulse oscillators promise (or have fulfilled, as for a Ti:sapphire oscillator) an outstanding scalability due to: i) reduced dispersion, ii) potentially broader spectra, and iii) rapid energy growth with the gain bandwidth in comparison with oscillators operating in the anomalous dispersion regime. One may hope, that a chirped-pulse oscillator is superior to an anomalous dispersion one in stability, starting-ability and noise properties and that sub- and over-100  $\mu\text{J}$  femtosecond pulse generation will be achievable directly from an oscillator as a result of development of this technique.

## 5. Acknowledgements

The research was funded by the Austrian Science Fund (FWF): P20293-N16.

## 6. References

- Ablowitz, M. J. & Horikis, T. P. (2009). Solitons in normally dispersive mode-locked lasers, *Phys. Rev. A* Vol. 79(No. 6): 063845.
- Agostini, P. & DiMauro, L. F. (2004). The physics of attosecond light pulses, *Rep. Prog. Phys.* Vol. 67(No. 6): 813–855.
- Agrawal, G. (2006). *Nonlinear Fiber Optics*, Academic, San Diego.

- Akhmediev, N. & Ankiewicz, A. (1997). *Solitons: Nonlinear Pulses and Beams*, Chapman & Hall, London.
- Akhmediev, N. & Ankiewicz, A. (eds) (2005). *Dissipative Solitons*, Springer, Berlin.
- Akhmediev, N. N. & Afanasjev, V. V. (1996). Singularities and special solutions of the cubic-quintic complex Ginzburg-Landau equation, *Phys. Rev. A* Vol. 53(No. 1): 1190–1201.
- Akhmediev, N., Soto-Crespo, J. M. & Grelu, P. (2008). Roadmap to ultra-short record high-energy pulses out of laser oscillator, *Physics Letters A* Vol. 372(No. 17): 3124–3128.
- Anderson, D., Lisak, M. & Berntson, A. (2001). A variational approach of nonlinear dissipative pulse propagation, *Pramana J. Phys.* Vol. 57(No. 5–6): 917–936.
- Ankiewicz, A., Akhmediev, N. & Devine, N. (2007). Dissipative solitons with a Lagrangian approach, *Optical Fiber Technology* Vol. 13(No. 2): 91–97.
- Apolonski, A., Poppe, A., Tempea, G., Spielmann, C., Udem, T., R. Holzwarth, Hänisch, T. & Krausz, F. (2000). Strong-field double ionization of Ar below the recollision threshold, *Phys. Rev. Lett.* Vol. 85(No. 4): 740–743.
- Aranson, I. S. & Kramer, L. (2002). The world of the complex Ginzburg-Landau equation, *Rev. Mod. Phys.* Vol. 74(No. 1): 99–143.
- Bale, B. G., Boscolo, S., Kutz, J. N. & Turitsyn, S. K. (2010). Intracavity dynamics in high-power mode-locked fiber lasers, *Phys. Rev. A* Vol. 81(No. 3): 033828.
- Bale, B. G., Boscolo, S. & Turitsyn, S. K. (2009). Dissipative dispersion-managed solitons in mode-locked lasers, *Opt. Lett.* Vol. 34(No. 21): 3286–3288.
- Bale, B. G. & Kutz, J. N. (2008). Variational method for mode-locked lasers, *J. Opt. Soc. Am. B* Vol. 25(No. 7): 1193–1202.
- Bale, B. G., Kutz, J. N., Chong, A., Renninger, W. H. & Wise, F. W. (2008a). Spectral filtering for high-energy mode-locking in normal dispersion fiber lasers, *J. Opt. Soc. Am. B* Vol. 25(No. 10): 1763–1770.
- Bale, B. G., Kutz, J. N., Chong, A., Renninger, W. H. & Wise, F. W. (2008b). Spectral filtering for mode-locking in the normal dispersive regime, *Opt. Lett.* Vol. 33(No. 9): 941–943.
- Bélangier, P.-A. (2007). Stable operation of mode-locked fiber lasers: similariton regime, *Optics Express* Vol. 15(No. 17): 11033–11041.
- Blanchard, P. & Brüning, E. (1992). *Variational Methods in Mathematical Physics: A Unified Approach*, Springer, Berlin.
- Brabec, T. & Krausz, F. (1997). Nonlinear optical pulse propagation in the single-cycle regime, *Phys. Rev. Lett.* Vol. 78(No. 17): 3282–3285.
- Brabec, T. & Krausz, F. (2000). Intense few-cycle laser fields: Frontiers of nonlinear optics, *Rev. Mod. Phys.* Vol. 72(No. 2): 545–591.
- Cankaya, H., Akturk, S. & Sennaroglu, A. (2011). Direct generation of 81 nJ pulses and external compression to a subpicosecond regime with a 4.9 MHz chirped-pulse multipass-cavity  $\text{Cr}^{4+}$ :forsterite oscillator, *Opt. Lett.* Vol. 36(No. 9): 1572–1574.
- Chang, W., Ankiewicz, A., Soto-Crespo, J. M. & Akhmediev, N. (2008a). Dissipative soliton resonance in laser models with parameter management, *J. Opt. Soc. Am. B* Vol. 25(No. 12): 1972–1977.
- Chang, W., Ankiewicz, A., Soto-Crespo, J. M. & Akhmediev, N. (2008b). Dissipative soliton resonances, *Phys. Rev. A* Vol. 78(No. 2): 023830.
- Chang, W., Soto-Crespo, J. M., Ankiewicz, A. & Akhmediev, N. (2009). Dissipative soliton resonances in the anomalous dispersion regime, *Phys. Rev. A* Vol. 79(No. 3): 033840.

- Cho, S. H., Bouma, B. E., Ippen, E. P. & Fujimoto, J. G. (1999). Low-repetition-rate high-peak-power Kerr-lens mode-locked Ti:Al<sub>2</sub>O<sub>3</sub> laser with a multiple-pass cavity, *Opt. Lett.* Vol. 24(No. 6): 417–419.
- Chong, A., Renninger, W. H. & Wise, F. W. (2008a). Properties of normal-dispersion femtosecond fiber lasers, *J. Opt. Soc. Am. B* Vol. 25(No. 2): 140–148.
- Chong, A., Renninger, W. H. & Wise, F. W. (2008b). Route to the minimum pulse duration in normal-dispersion fiber lasers, *Opt. Lett.* Vol. 33(No. 22): 2638–2640.
- Conte, R. (ed.) (1999). *The Painlevé Property. One Century Later*, Springer, New York.
- Deissler, R. J. & Brand, H. R. (1994). Periodic, quasiperiodic, and chaotic localized solutions of the quintic complex Ginzburg-Landau equation, *Phys. Rev. Lett.* Vol. 72(No. 4): 478–481.
- der Au, J. A., Spühler, G. J., Südmeyer, T., Paschotta, R., Hövel, R., Moser, M., Erhard, S., Karzewski, M., Gissen, A. & Keller, U. (2000). 16.2-W average power from a diode-pumped femtosecond Yb:YAG thin disk laser, *Opt. Lett.* Vol. 25(No. 11): 859–861.
- Diels, J.-C. & Rudolph, W. (2006). *Ultrashort Laser Pulse Phenomena: Fundamentals, Techniques, and Applications on a Femtosecond Time Scale*, Elsevier, Amsterdam.
- Ding, E. & Kutz, J. N. (2009). Operating regimes, split-step modeling, and the Haus master mode-locking model, *J. Opt. Soc. Am. B* Vol. 26(No. 12): 2290–2300.
- Fernandez, A., Fuji, T., Poppe, A., Fürbach, A., Krausz, F. & Apolonski, A. (2004). Chirped-pulse oscillators: a route to high-power femtosecond pulses without external amplification, *Opt. Lett.* Vol. 29(No. 12): 1366–1368.
- Fernández, A., Verhoef, A., Pervak, V., Lermann, G., Krausz, F. & Apolonski, A. (2007). Generation of 60-nJ sub-40-fs pulses at 70 MHz repetition rate from a Ti:sapphire chirped pulse-oscillator, *Appl. Phys. B* Vol. 87(No. 3): 395–398.
- Fernández González, A. (2008). *Chirped-Pulse Oscillators: Generating Microjoule Femtosecond Pulses at Megahertz Repetition Rate*, VDM Verlag.
- Gattass, R. R. & Mazur, E. (2008). Femtosecond laser micromachining in transparent materials, *Nature Photonics* Vol. 2(No. 4): 219–225.
- Giessen, A. & Speiser, J. (2007). Fifteen years of work on thin-disk lasers: results and scaling laws, *IEEE J. Selected Top. in Quantum. Electron.* Vol. 13(No. 3): 598–609.
- Grely, P., Chang, W., Ankiewicz, A., Soto-Crespo, J. M. & Akhmediev, N. (2010). Dissipative soliton resonance as a guideline for high-energy pulse laser oscillators, *J. Opt. Soc. Am. B* Vol. 27(No. 11): 2336–2341.
- Hannaford, P. (ed.) (2005). *Femtosecond Laser Spectroscopy*, Springer, Boston.
- Haus, H. A. (1975a). Theory of mode locking with a fast saturable absorber, *J. Applied Phys.* Vol. 46(No. 7): 3049–3058.
- Haus, H. A. (1975b). Theory of mode locking with a slow saturable absorber, *IEEE J. Quantum Electron.* Vol. 11(No. 9): 736–746.
- Haus, H. A., Fujimoto, J. G. & Ippen, E. P. (1991). Structures for additive pulse mode locking, *J. Opt. Soc. Am. B* Vol. 8(No. 10): 2068–2076.
- Haus, H. A. & Silberberg, Y. (1985). Theory of mode locking of a laser diode with a multiple-quantum-well structure, *J. Opt. Soc. Am. B* Vol. 2(No. 7): 1237–1243.
- Herrmann, J. & Wilhelmi, B. (1987). *Lasers for ultrashort light pulses*, Elsevier, Amsterdam.
- Horowitz, M., Barad, Y. & Silberberg, Y. (1997). Noiselike pulses with a broadband spectrum generated from an erbium-doped fiber laser, *Opt. Lett.* Vol. 22(No. 11): 799–801.

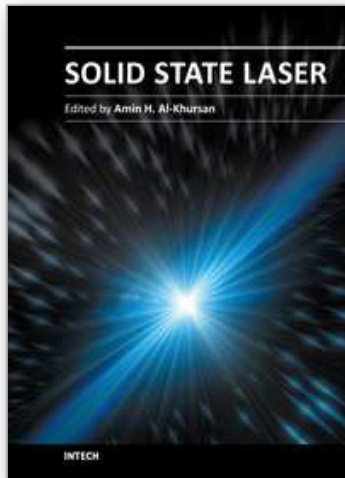
- Huber, R., Adler, F., Leitenstorfer, A., Beutler, M., Baum, P. & Riedle, E. (2003). 12-fs pulses from a continuous-wave-pumped 200-nJ Ti:sapphire amplifier at a variable repetition rate as high as 4 MHz, *Opt. Lett.* Vol. 28(No. 21): 2118–2120.
- Jasapara, J., Kalashnikov, V. L., Krimer, D. O., Poloyko, I. G., Lenzner, M. & Rudolph, W. (2000). Automodulations in cw Kerr-lens mode-locked solid-state lasers, *J. Opt. Soc. Am. B* Vol. 17(No. 2): 319–326.
- Jirauschek, C. & Kärtner, F. X. (2006). Gaussian pulse dynamics in gain media with Kerr nonlinearity, *J. Opt. Soc. Am. B* Vol. 23(No. 9): 1776–1784.
- Kalashnikov, V. & Apolonski, A. (2010). Energy scalability of mode-locked oscillators: a completely analytical approach to analysis, *Optics Express* Vol. 18(No. 24): 25757–25770.
- Kalashnikov, V. L. (2003). Propagation of the gaussian ultrashort pulse in a nonlinear laser medium. Commented Maple computer algebra worksheet, available at <http://info.tuwien.ac.at/kalashnikov/selfff.html>.
- Kalashnikov, V. L. (2008). Chirped-pulse oscillators: an impact of the dynamic gain saturation. Preprint arXiv:0807.1050v1 [physics.optics], available at <http://lanl.arxiv.org/abs/0807.1050>.
- Kalashnikov, V. L. (2009a). Chirped dissipative solitons of the complex cubic-quintic nonlinear Ginzburg-Landau equation, *Phys. Rev. E* Vol. 80(No. 4): 046606.
- Kalashnikov, V. L. (2009b). The unified theory of chirped-pulse oscillators, in M. Bertolotti (ed.), *Proc. SPIE: Nonlinear Optics and Applications III*, Vol. 7354, SPIE, p. 73540T.
- Kalashnikov, V. L. (2010). Chirped dissipative solitons, in L. F. Babichev & V. I. Kuvshinov (eds), *Nonlinear Dynamics and Applications*, Vol. 16, Republic Institute of Higher School, Minsk, pp. 199–206.
- Kalashnikov, V. L. (2011). Dissipative solitons: Perturbations and chaos formation, in C. H. Skiadas, I. Dimotikalis & C. Skiadas Babichev (eds), *Chaos Theory. Modeling, Simulation and Applications*, World Scientific Publishing Company, London, pp. 58–67.
- Kalashnikov, V. L. & Apolonski, A. (2009). Chirped-pulse oscillators: A unified standpoint, *Phys. Rev. A* Vol. 79(No. 4): 043829.
- Kalashnikov, V. L. & Chernykh, A. (2007). Spectral anomalies and stability of chirped-pulse oscillators, *Phys. Rev. A* Vol. 75(No. 3): 033820.
- Kalashnikov, V. L., Fernández, A. & Apolonski, A. (2008). High-order dispersion in chirped-pulse oscillators, *Optics Express* Vol. 16(No. 6): 4206–4216.
- Kalashnikov, V. L., Kalosha, V. P., Mikhailov, V. P. & Poloyko, I. G. (1995). Self-mode locking of four-mirror-cavity solid-state lasers by Kerr self-focusing, *J. Opt. Soc. Am. B* Vol. 12(No. 3): 462–467.
- Kalashnikov, V. L., Kalosha, V. P., Mikhailov, V. P., Poloyko, I. G., Demchuk, M. I., Koltchanov, I. G. & Eichler, H. J. (1995). Frequency-shift mode locking of continuous-wave solid-state lasers, *J. Opt. Soc. Am. B* Vol. 12(No. 11): 2078–2082.
- Kalashnikov, V. L., Podivilov, E., Chernykh, A. & Apolonski, A. (2006). Chirped-pulse oscillators: theory and experiment, *Applied Physics B* Vol. 83(No. 4): 503–510.
- Kalashnikov, V. L., Podivilov, E., Chernykh, A., Naumov, S., Fernandez, A., Graf, R. & Apolonski, A. (2005). Approaching the microjoule frontier with femtosecond laser oscillators: theory and comparison with experiment, *New Journal of Physics* Vol. 7(No. 1): 217.
- Kalashnikov, V. L., Sorokin, E. & Sorokina, I. T. (2011). Chirped dissipative soliton absorption spectroscopy, *Optics Express* Vol. 19(No. 18): 17480–17492.

- Kalosha, V. P., Müller, M., Herrmann, J. & Gatz, S. (1998). Spatiotemporal model of femtosecond pulse generation in Kerr-lens mode-locked solid-state lasers, *J. Opt. Soc. Am. B* Vol. 15(No. 2): 535–550.
- Kärtner, F. X., Morgner, U., Schibli, T., Ell, R., Haus, H. A., Fujimoto, J. G. & Ippen, E. P. (2004). Few-cycle pulses directly from a laser, in F. X. Kärtner (ed.), *Few-cycle laser pulse generation and its applications*, Springer, Berlin, pp. 73–136.
- Keller, U., Weingarten, K. J., Kärtner, F. X., Kopf, D., Braun, B., Jung, I. D., Fluck, R., Hönninger, C., Matuschek, N. & J. A. d. A. (1996). Semiconductor saturable absorber mirrors (SESAMs) for femtosecond to nanosecond pulse generation in solid-state lasers, *IEEE J. Sel. Top. Quantum Electron.* Vol. 2(No. 3): 435–453.
- Kharenko, D. S., Shtyrina, O. V., Yarutkina, I. A., Podivilov, E. V., Fedoruk, M. P. & Babin, S. A. (2011). Highly chirped dissipative solitons as a one-parameter family of stable solutions of the cubic-quintic Ginzburg-Landau equation, *J. Opt. Soc. Am. B* Vol. 28(No. 10): 2314–2319.
- Koehnner, W. (2006). *Solid-State Laser Engineering*, Springer, New York.
- Komarov, A., Leblond, H. & Sanchez, F. (2005). Quantic complex Ginzburg-Landau model for ring fiber laser, *Phys. Rev. E* Vol. 72(No. 2): 025604(R).
- Krausz, F. & Ivanov, M. (2009). Attosecond physics, *Rev. Mod. Phys.* Vol. 81(No. 1): 163–234.
- Lecaplain, C., Baumgartl, M., Schreiber, T. & Hideur, A. (2011). On the mode-locking mechanism of a dissipative-soliton fiber oscillator, *Optics Express* Vol. 19(No. 27): 26742–26751.
- Lin, J-H. & Lin, K-H. (2010). Multiple pulsing and harmonic mode-locking in an all-normal-dispersion Nd:GdO<sub>4</sub> laser using a nonlinear mirror, *J. Phys. B*. Vol. 43(No. 6): 065402.
- Liu, X. (2010). Pulse evolution without wave breaking in a strongly dissipative dispersive laser system, *Phys. Rev. A* Vol. 81(No. 5): 053819.
- Liu, Y., Tschuch, S., Rudenko, A., Dürr, M., Siegel, M., Morgner, U., Moshhammer, R. & Ullrich, J. (2008). Strong-field double ionization of air below the recollision threshold, *Phys. Rev. Lett.* Vol. 101(No. 5).
- Maimistov, A. I. (1993). Evolution of solitary waves which are approximately solitons of a nonlinear Schrödinger equation, *J. Exp. Theor. Phys.* Vol. 77(No. 5): 727–731.
- Malomed, B. A. (2002). Variational methods in nonlinear fiber optics and related fields, in E. Wolf (ed.), *Variational methods in nonlinear fiber optics and related fields*, Vol. 43, Elsevier, Amsterdam, pp. 71–193.
- Malomed, B. A. & Nepomnyashchy, A. A. (1990). Kinks and solitons in the generalized Ginzburg-Landau equation, *Phys. Rev. A* Vol. 42(No. 10): 6009–6014.
- Martin, M. M. & Hynes, J. T. (eds) (2003). *Femtochemistry and femtobiology: ultrafast events in molecular science*, Elsevier, Amsterdam.
- Mourou, G. A., Tajima, T. & Bulanov, S. V. (2006). Optics in the relativistic regime, *Rev. Mod. Phys.* Vol. 78(No. 2): 309–692.
- Naumov, S., Fernandez, A., Graf, R., Dombi, P. & Apolonski, F. K. A. (2005). Approaching the microjoule frontier with femtosecond laser oscillators, *New Journal of Physics* Vol. 7(No. 1): 216.
- Oughstun, K. E. (2009). *Electromagnetic and Optical Pulse Propagation 2: Temporal Pulse Dynamics in Dispersive, Attenuative Media*, Springer.

- Palmer, G., Schultze, M., Siegel, M., Emons, M., Bünding, U. & Morgner, U. (2008). Passively mode-locked Yb:KLu(WO<sub>4</sub>)<sub>2</sub> thin-disk oscillator operated in the positive and negative dispersion regime, *Opt. Lett.* Vol. 33(No. 14): 1608–1610.
- Palmer, G., Schultze, M., Siegel, M., Emons, M., Lindemann, A. L., Pospiech, M., Steingrube, D., Lederer, M. & Morgner, U. (2010). 12 MW peak power from a two-crystal Yb:KYW chirped-pulse oscillator with cavity-dumping, *Optics Express* Vol. 18(No. 18): 19095–19100.
- Paschotta, R. (2008). *Encyclopedia of Laser Physics and Technology*, Wiley.
- Perez-Garcia, V. M., Torres, P. & Montesinos, G. D. (2007). The method of moments for nonlinear Schrödinger equations: theory and applications, *SIAM J. Appl. Math.* Vol. 67(No. 4): 990–1015.
- Pervak, V., Teisset, C., Siguta, A., Naumov, S., Krausz, F. & Apolonski, A. (2008). High-dispersive mirrors for femtosecond lasers, *Optics Express* Vol. 16(No. 14): 10220–10233.
- Pfeifer, T., Spielmann, C. & Gerber, G. (2006). Femtosecond X-ray science, *Rep. Prog. Phys.* Vol. 69(No. 2): 443–505.
- Podivilov, E. & Kalashnikov, V. L. (2005). Heavily-chirped solitary pulses in the normal dispersion region: new solutions of the cubic-quintic complex Ginzburg-Landau equation, *JETP Letters* Vol. 82(No. 8): 467–471.
- Proctor, B., Westwig, E. & Wise, F. (1993). Characterization of a Kerr-lens mode-locked Ti:sapphire laser with positive group-velocity dispersion, *Opt. Lett.* Vol. 18(No. 19): 1654–1656.
- Renninger, W. H., Chong, A. & Wise, F. W. (2008). Dissipative solitons in normal-dispersion fiber lasers, *Phys. Rev. A* Vol. 77(No. 2): 023814.
- Renninger, W. H., Chong, A. & Wise, F. W. (2011). Pulse shaping and evolution in normal-dispersion mode-locked fiber lasers, *IEEE J. Sel. Top. Quantum Electron.* Vol. PP(No. 99): DOI:10.1109/JSTQE.2011.2157462.
- Rühl, A. (2008). *The normal dispersion regime in passively mode-locked fiber oscillators*, Cuvillier Verlag, Göttingen.
- Siegel, M., Palmer, G., Emons, M., Schultze, M., Ruchl, A. & Morgner, U. (2008). Pulsing dynamics in Ytterbium based chirped-pulse oscillator, *Optics Express* Vol. 16(No. 19): 14314–14320.
- Siegel, M., Pfullmann, N., Palmer, G., Rausch, S., Binhammer, T., Kovacev, M. & Morgner, U. (2009). Microjoule pulse energy from a chirped-pulse Ti:sapphire oscillator with cavity dumping, *Opt. Lett.* Vol. 34(No. 6): 740–742.
- Sorokin, E., Kalashnikov, V. L., Mandom, J., Guelachvili, G., Picquè, N. & Sorokina, I. T. (2008). Cr<sup>4+</sup>:YAG chirped-pulse oscillator, *New Journal of Physics* Vol. 10(No. 8): 083022.
- Sorokina, I. T. (2003). Crystalline mid-infrared lasers, in I. T. Sorokina & V. K. L. (eds), *Solid-state mid-infrared laser sources*, Springer-Verlag, Berlin, pp. 255–349.
- Soto-Crespo, J. M., Akhmediev, N. N., Afanasjev, V. V. & Wabnitz, S. (1997). Pulse solutions of the cubic-quintic complex Ginzburg-Landau equation in the case of normal dispersion, *Phys. Rev. E* Vol. 55(No. 4): 4783–4796.
- Soto-Crespo, J. M., Akhmediev, N. & Town, G. (2002). Continuous-wave versus pulse regime in a passively mode-locked laser with a fast saturable absorber, *J. Opt. Soc. Am. B* Vol. 19(No. 2): 234–242.
- Spence, D. E., Kean, P. N. & Sibbett, W. (1991). 60-fsec pulse generation from a self-mode-locked Ti:sapphire laser, *Opt. Lett.* Vol. 16(No. 1): 42–44.

- Spence, D. E. & Sibbett, W. (1991). Femtosecond pulse generation by a dispersion-compensated, coupled-cavity, mode-locked Ti:sapphire laser, *J. Opt. Soc. Am. B* Vol. 18(No. 19): 2053–2060.
- Steinmeyer, G., Sutter, D. S., Gallmann, L., Matuschek, N. & Keller, U. (1999). Frontiers in ultrashort pulse generation: pushing the limits in linear and nonlinear optics, *Science* Vol. 286(No. 19): 1507–1512.
- Südmeyer, T., Kränkel, C., Baer, C. R. E., Heckl, O. H., Saraceno, C. J., Golling, M., Peters, R., Petermann, K., Huber, G. & Keller, U. (2009). High-power ultrafast thin disk laser oscillators and their potential for sub-100-femtosecond pulse generation, *Appl. Phys. B* Vol. 97(No. 2): 281–295.
- Südmeyer, T., Marchese, S. V., Hashimoto, S., Baer, C. R. E., Gingras, G., Witzel, B. & Keller, U. (2008). Femtosecond laser oscillators for high-field science, *Nature Photonics* Vol. 2(No. 10): 599–604.
- Tan, W. D., Tang, D. Y., Xu, C. W., Zhang, J., Xu, X. D., Li, D. Z. & Xu, J. (2011). Evidence of dissipative solitons in  $\text{Yb}^{3+}:\text{CaYAlO}_4$ , *Optics Express* Vol. 36(No. 19): 18495–18500.
- Tsoy, E. N. & Akhmediev, N. N. (2005). Bifurcations from stationary to pulsating solitons in the cubic-quintic complex Ginzburg-Landau equation, *Physics Letters A* Vol. 343(No. 6): 417–422.
- Tsoy, E. N., Ankiewicz, A. & Akhmediev, N. (2006). Dynamical models for dissipative localized waves of the complex Ginzburg-Landau equation, *Phys. Rev. E* Vol. 73(No. 3): 036621.
- Usechak, N. G. & Agrawal, G. P. (2005). Semi-analytic technique for analyzing mode-locked lasers, *Optics Express* Vol. 13(No. 6): 2075–2081.
- van Saarloosa, W. & Hohenberg, P. C. (1992). Fronts, pulses, sources and sinks in generalized complex Ginzburg-Landau equations, *Physica D: Nonlinear Phenomena* Vol. 56(No. 4): 303–367.
- Weiner, A. M. (2009). *Ultrafast Optics*, Wiley.
- Wise, F. W., Chong, A. & Renninger, W. H. (2008). High-energy femtosecond fiber lasers based on pulse propagation at normal dispersion, *Laser & Photon. Rev.* Vol. 2(No. 1–2): 58–73.
- Zhavoronkov, N., Maekawa, H., Okuno, H. & Tominaga, K. (2005). All-solid-state femtosecond multi-kilohertz laser system based on a new cavity-dumped oscillator design, *J. Opt. Soc. Am. B* Vol. 22(No. 3): 567–571.

IntechOpen



### **Solid State Laser**

Edited by Prof. Amin Al-Khursan

ISBN 978-953-51-0086-7

Hard cover, 252 pages

**Publisher** InTech

**Published online** 17, February, 2012

**Published in print edition** February, 2012

This book deals with theoretical and experimental aspects of solid-state lasers, including optimum waveguide design of end pumped and diode pumped lasers. Nonlinearity, including the nonlinear conversion, up frequency conversion and chirped pulse oscillators are discussed. Some new rare-earth-doped lasers, including double borate and halide crystals, and feedback in quantum dot semiconductor nanostructures are included.

#### **How to reference**

In order to correctly reference this scholarly work, feel free to copy and paste the following:

Vladimir L. Kalashnikov (2012). Chirped-Pulse Oscillators: Route to the Energy-Scalable Femtosecond Pulses, Solid State Laser, Prof. Amin Al-Khursan (Ed.), ISBN: 978-953-51-0086-7, InTech, Available from: <http://www.intechopen.com/books/solid-state-laser/chirped-pulse-oscillators-a-route-to-the-energy-scalable-femtosecond-pulses>

**INTECH**  
open science | open minds

#### **InTech Europe**

University Campus STeP Ri  
Slavka Krautzeka 83/A  
51000 Rijeka, Croatia  
Phone: +385 (51) 770 447  
Fax: +385 (51) 686 166  
[www.intechopen.com](http://www.intechopen.com)

#### **InTech China**

Unit 405, Office Block, Hotel Equatorial Shanghai  
No.65, Yan An Road (West), Shanghai, 200040, China  
中国上海市延安西路65号上海国际贵都大饭店办公楼405单元  
Phone: +86-21-62489820  
Fax: +86-21-62489821

© 2012 The Author(s). Licensee IntechOpen. This is an open access article distributed under the terms of the [Creative Commons Attribution 3.0 License](#), which permits unrestricted use, distribution, and reproduction in any medium, provided the original work is properly cited.

IntechOpen

IntechOpen